ELECTRON-ION COINCIDENCE STUDIES OF Kr, Xe, N$_2$ AND CO
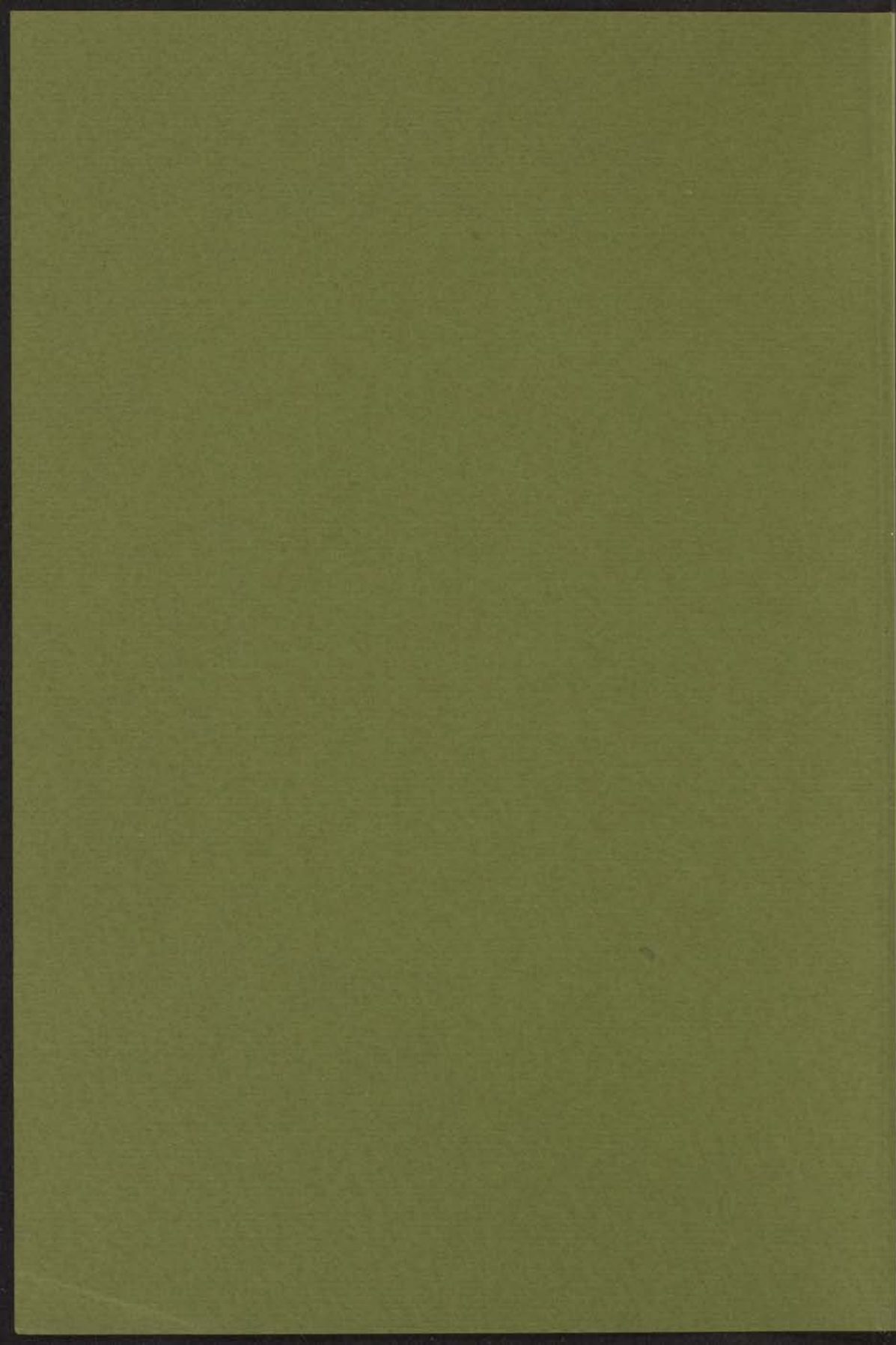
Th. M. EL-SHERBINI

ELECTRON-ION COINCIDENCE STUDIES
OF Kr, Xe, N$_2$ AND CO

ELECTRON-ION COINCIDENCE STUDIES OF Kr, Xe, N₂ AND CO

DOOR

THARWAT MAHMOUD EL-SHERBINI

GEBOREN TE CAIRO (EGYPTE) IN 1942

PROMOTOR : Prof. Dr. J. Kistemaker

CO-REFERENT: Dr. F.J.de Heer

Dit proefschrift kwam tot stand onder toezicht
en leiding van Dr. M.J.van der Wiel

To my parents

PROPOSITIONS

I

In order to predict the correct values of the photo-absorption cross sections at the 3d threshold of Kr and the 4d threshold of Xe, one should consider contributions from the 4p-ϵd and 5p-ϵd maxima of Kr and Xe respectively as well as simultaneous processes in the outer- and first inner shells of the two gases.

- Cooper, J.W., Phys.Rev.Letters 13 (1964) 762.
- Amusia, M.Ya., Cherepkov, N.A. and Chernysheva, L.V., Soviet Physics - JETP 33 (1971) 90.
- This thesis chapter II.

II

The model applied by Van der Wiel and Wiebes in order to obtain the "shake-off" probability for the ejection of M electrons of an Ar-atom in the case of the creation of an L hole as well as in the case of filling this hole, is not correct for the latter case.

- Van der Wiel, M.J. and Wiebes, G., Physica 53 (1971) 225.

III

An upper limit to the lifetime of the predissociated
levels of the N_2^+-state at the first dissociation limit
is about 20 nsec. The identification of this state
with the $C^2\Sigma_u^+$ state of N_2^+ is questionable, even though
the above upper limit is in agreement with the life-
time of these levels as determined by Fournier et al.

- This thesis Chapter III.
- Fournier, P., Van de Runstraat, C.A., Govers, T.R.,
  Schopman, J., de Heer, F.J. and Los, J., Chem.Phys.
  Letters <u>9</u> (1971) 426.

IV

The conclusion of Hayden Smith that the light emission
between 2400 and 2600 Å formed by electron impact on
SO_2 is only due to SO_2 molecule is doubtful.

- Hayden Smith, W., J.Quant.Spectry.Radiative Trans-
  fer <u>9</u> (1969) 1191.

V

Stalherm et al. and Carlson et al. observed a peak at
383.8 eV and one at 384.7 eV in the Auger electron
spectrum of N_2. Their interpretation of these peaks
as being due to the decay of the $(\sigma_u 1s)^1 (\Pi_g 2p)^1$,
$^1\Pi_u$ excited state to the $A^2\Pi_u$, $\hat{v} = 0$ (or 1) and
$X^2\Sigma_g^+$, $\hat{v} = 0$ states of N_2^+, is in contradiction with

the shape of the potential energy curve of this excited
state suggested by the results of Nakamura et al.

- Stalherm, D., Cleff, B., Hillig, H. and Mehlhorn, W.,
  Z.Naturforsch. 24a (1969) 1728.
- Carlson, T.A., Moddeman, W.E., Pullen, B.P. and
  Krause, M.O., Chem.Phys.Letters 5 (1970) 390.
- Nakamura, M., Sasanuma, M., Sato, S., Watanabe, M.,
  Yamashita, H., Iguchi, Y., Ejiri, A., Nakai, S.,
  Yamaguchi, S., Sagawa, T., Nakai, Y. and Oshio, T.,
  Phys.Rev. 178 (1969) 80.
- This thesis Chapter III.

VI

The photo-electron method showed a displacement in the
photo-electron line from its ideal position which has been
attributed to the inelastic energy losses suffered by
the photo-electrons when leaving the bulk of the crystal.
In addition to this effect however one may expect that
the binding energies of electrons in the bulk of the crys-
tal differs from those at the surface. Such a difference
can be measured by the method proposed by Brahm Dev and
H. Brinkman.

- Nordling, C., Arkiv Fysik 6 (1959) 397.
- Brahm Dev and Brinkman, H., Paper III.6 International
  Symposium on Surface Physics and Ultra-high Vacuum
  science and Technology, Groningen, september 1970.

VII

To obtain more information about excited states in atoms
and molecules, the present study can be extended by observing
the radiative decay of these states. This is possible by
modifying our apparatus in such a way that coincidences
between scattered electrons, ions and photons can be detected.

VIII

By making use of existing calculations on inner shell
ionization of atoms by electron impact using Hartree-Fock
Slater wave functions it can be shown that in the Born
region, the proton impact cross-sections obtained by
Khandelwal, Choi and Merzbacher are 30% too high.

- Khandelwal, G.S., Choi, B.H. and Merzbacher, E.,
  Atomic Data 1 (1969) 103.

IX

In western and non-western countries alike it is not
sufficiently realized that scientific and technological
aid in training and investment should be accompanied by
an adequate endeavour in the field of comparative
anthropology, which may be profitable to both parties
eventually.

Th.M. El-Sherbini   Leyden, 17 May 1972.

CONTENTS

CHAPTER I

INTRODUCTION

1. *General*. Excitation of atoms and molecules and the subsequent
ionization and fragmentation has received special attention by many in-
vestigators in the last few years. A considerable amount of quantita-
tive and detailed information in this field has been gained with the
progress of the various experimental techniques. Among these techniques
are:

a) The photoabsorption technique, in which the attenuation of a photon
   beam after passing through a gaseous target is measured. With this
   technique, very high energy resolution can be obtained as shown in
   investigations[1,2,3] on the excited states of atoms and molecules.
   The energy range is greatly extended by the use of line sources[4],
   at the expense of continuous energy variation. However, a continu-
   ous energy source extending far into the vacuum ultraviolet and
   X-ray region is now available by the use[5] of electron synchrotron
   radiation.

b) The photoionization technique, in which a mass spectrometric study
   is carried out of the various ions produced after ionizing the gas
   with a photon beam. This technique yields valuable data[6,7,8] with
   respect to single as well as to multiple ionization (and to disso-
   ciative ionization in case of molecules).

c) Photoelectron spectroscopy, in which the kinetic energies of the
   photo-ejected electrons from atoms and molecules are measured. This
   technique has been extensively developed[9,10,11] for the study of
   electron orbital energies of atoms and molecules. It gives informa-
   tion only about states excited in the initial energy absorption.

d) Auger electron spectroscopy, in which the energies (and intensities)

of electrons ejected as a result of a non-radiative readjustment
to an inner-shell vacancy (this vacancy can either be created in
an atom or a molecule by photon or electron impact), are measured.
This technique was used in investigating the decay processes follow-
ing the creation of inner-shell vacancies in atoms[12] and recently
[11,13] in determining the electronic states of doubly ionized mole-
cules. However it only provides energy differences and unambiguous
assignment of the initial and final states is not always possible.

The work presented in this thesis was done using a method which has
recently been developed[14] and proved a valuable tool in the study of
multiple ionization of He, Ne and Ar. In this method which is most clo-
sely related to that of photoionization (b), the use of a photon source
of variable energy is simulated by measuring the energy loss of fast
electrons (10 keV), scattered at a small angle, and the relation between
energy transfer and ion formation is determined by coincidence detection
of the scattered electron and the corresponding ion. This technique of-
fers the advantages of a continuously variable energy transfer (energy
loss) over a wide range (0 - 500 eV) together with a constant detection
efficiency. Only one calibration point is needed to obtain absolute
values in the whole energy range. Moreover the intensity is sufficient
to permit the use of a low target gas density ($\sim 10^{-5}$ torr) such that ex-
traction of ions and separation of charge states is feasible. This forms
a further advantage of a possible alternative of charge analysis of ions
formed by dispersed electron synchrotron radiation.

It is of interest to study the two noble gases Kr and Xe since due to
the proximity of the outer and first inner shells a great deal about
the role played by electron correlation effects in multiple ionization
of atoms may be revealed. In this context one should remark that the
discrepancies[15,16] which exist between experiment and theory for the
photoionization cross sections of the 3d electrons in Kr and the 4d
electrons in Xe, may be due to these correlation effects which have been
neglected in the calculations (see ref.17).

For the two isoelectronic diatomic molecules N_2 and CO the primary
aim of our study is to investigate the various processes involving
outer-shell as well as K-shell excitations and their subsequent ioniza-
tion and dissociation. Furthermore we want to compare our results with
those in literature since a vast amount of information on these mole-
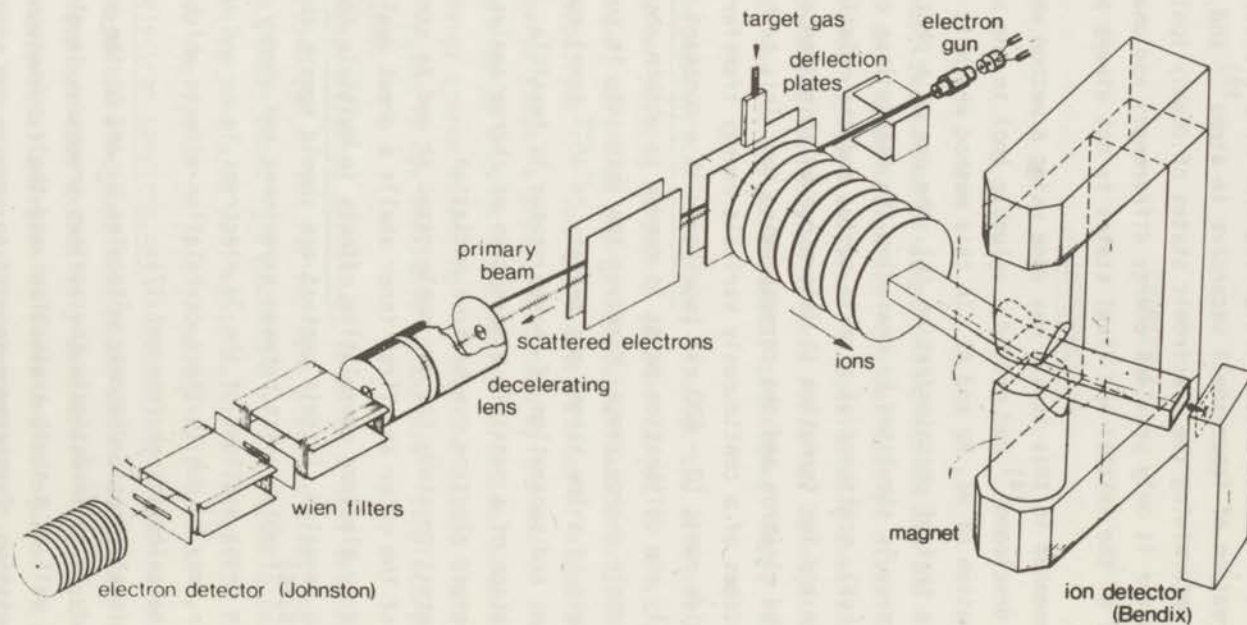
Fig.1. Schematic view of the scattered electron-ion coincidence apparatus.

cules is already available. Such a comparison can lead to more detailed knowledge about these processes (see ref.18).

2. *Apparatus and electronics*. A schematic view of the scattered electron-ion coincidence apparatus is shown in fig.1. The main components of the apparatus are:

2.1. *The electron source*. The electron source is a Philips 6-AW-59 electron gun from a television tube. It consist of an oxide coated cathod ($B_a O$), Wehnelt cylinder, anode, and electrostatic focusing lens.

The electron beam from the gun has an 0.5 mm diameter in the collision region. The effect of the earth magnetic field on the path of the electrons was eliminated by surrounding the apparatus with compensation coils.

2.2. *The collision region*. Collisions occur in the intersection of the electron beam (0.5 mm diameter) with the neutral beam of gas atoms (1 × 8 mm) emerging from a multi-channel gas jet.

Ions are extracted from the collision region by a homogeneous extraction field (50 - 600 V/cm), produced by electrodes, with slits much larger than the ion beam dimensions, see fig.1. This design of the extraction electrodes allows all the ions formed with thermal energies to be extracted.

2.3. *The energy selector*. After collision all electrons accepted by the 1 mm diameter angular selection hole at 200 mm from the collision centre, see fig.1, are decelerated by a deceleration lens to an energy between 20 and 100 eV and then energy analyzed with a resolution of 1 to 5 eV fwhm by the crossed field energy selector (a double Wien filter).

Each Wien filter is composed of two electrostatic plates, 6 cm length and 1.25 cm separation, surrounded by two 6 turns electric coils which give the perpendicular magnetic field. The magnetic field can be changed from 0 to 20 gauss. After the double Wien filter the electrons are post-accelerated up to 200 eV and then hit the electron detector.

2.4. *The mass spectrometer*. Our mass spectrometer which acts in fact as a charge analyzer was designed to give 100% transmission in combination with the extraction system, for ions formed with zero excess energy. It consists of a 30° magnet with a magnetic field up to 3500 gauss and an analyzer tube of 40 cm length, see fig.1.

The stray field of the analyzer magnet at the electron beam path was reduced to less than 10^{-2} gauss by shielding the magnet with a layer of iron and one of "Co Netic".

The charge resolving power of the system is 1:8. After the analyzer the ions are post-accelerated to about 7 keV and then hit the ion detector.

2.5. *The vacuum system*. The vacuum system consists of four oil diffusion pumps, two of them for the collision chamber (one at the side of the gas inlet and the other at the ion extraction side) and the other two under the Wien filters and the mass spectrometer. Liquid air cooled baffles are used above the pump under the Wien filter to prevent the oil vapour to come into the apparatus.

Thermo-electrically cooled Chevron baffles are used for the same purpose on the other pumps.

The fore-vacuum is attained by a two stage rotary high-vacuum pump which gives an ultimate pressure of 10^{-4} Torr. This fore-vacuum is separated from the high vacuum by a small diffusion pump which brings the pressure down to 10^{-5} torr and prevents the oil of the rotary pump from entering the high-vacuum.

The space containing the electron detector which can be shut off from the rest of the apparatus by a valve, is pumped by an 8 litre/sec ionization pump which gives a clean and a high-vacuum ($\sim 10^{-9}$ torr).

The relative pressures in the space containing the collision region and the Wien filters are measured with two ionization gauges.

The background pressure is 5×10^{-8} torr, and when target gas is introduced it rises to about 1×10^{-6} torr.

2.6. *Detectors*. The electron detector is a Johnston Focused Mesh Multiplier (model MM-1), and the ion detector is a Bendix M-306 Magnetic Multiplier. Each detector is connected to a 50 Ω input solid state current amplifier (voltage gain of 1600 at 4 n sec rise time).

The counting efficiency for electrons is about 80% with a background of about 1 pulse/sec., while for ions it is 100% with a background of about 1 pulse/5 min. The efficiency for ions was confirmed to an accuracy of 10% by a DC-measurement. The output pulses from the electron and the ion detector are measured in delayed coincidence.

2.7. *The coincidence circuit*. The block diagram of the coincidence circuit is shown in fig.2. Channel 1 and channel 2 in the figure represent the ion and electron channels respectively. The pulses in the electron channel are fed into two separate delay units, consisting of a set of 50 Ω coaxial cables with pulse shapers at the input and output ends, in order to detect coincidences simultaneously at two positions
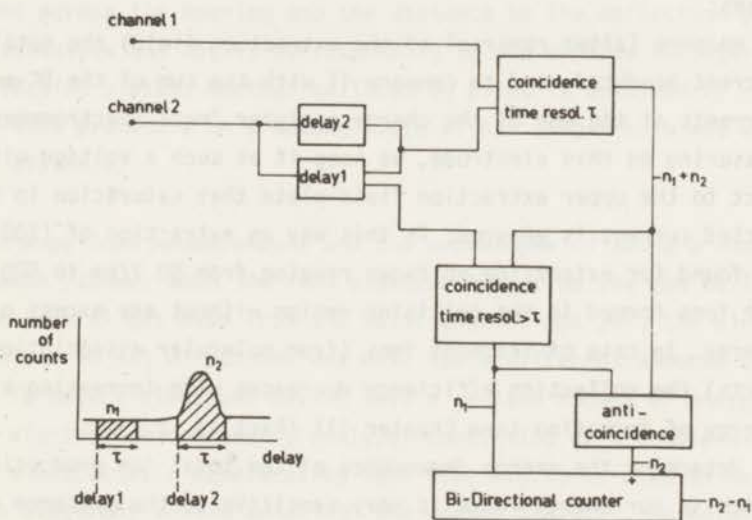
Fig.2.   Block diagram of the coincidence circuit.
Inset: usual distribution of true and accidental coincidences present in two partly correlated detector signals.

in the delay spectrum (see inset of fig.2): accidental coincidences n_1 are measured at delay 1 and true plus accidental ones n_2 at delay 2. Since coincidences from the two delay positions 1 and 2 are measured by one coincidence gate, the effective time resolutions for both delay setting are the same. The separation of the counts n_1 from n_2 is performed with an identifier system, consisting of a coincidence and an anticoincidence gate both with time resolutions larger than the first gate (see fig.2). The output of these gates are connected to a

bidirectional counter, which subtracts the two signals n_1 and n_2 to give the number of true coincidences.

3. *Experimental procedure*. In this section we shall discuss some experimental procedures.

3.1. *Extraction of ions*. A highly insulated electrode has been placed behind a slit in the upper extraction field plate (see fig.1) for two purposes:

a) To measure (after reversal of the extraction field) the total ion current produced, and to compare it with the sum of the DC-measured currents at the end of the charge analyzer "mass spectrometer". When measuring on this electrode, we keep it at such a voltage with respect to the upper extraction field plate that saturation in the collected current is ensured. In this way an extraction of $(100 \pm 3)\%$ is found for extraction voltages ranging from 50 V/cm to 600 V/cm for ions formed in the collision region without any excess of kinetic energy. In case of. fragment ions (from molecular dissociation products) the collection efficiency decreases with increasing kinetic energy of formation (see Chapter III (Part A), 2.2).

b) To determine the energy dependence of the total ion production, which in our energy range is very sensitive to the presence of secondary electrons. After normalization at 10 keV a check on Ar showed [19] a 3% reproduction of Schram's gross ionization data[20], which we believe to be free from secondary electron effects. Suppression of effects due to secondary electrons in our apparatus is easy due to the abscence of an axial magnetic field in the ionization chamber.

Since the electron beam is deflected in the ion extraction region, we have to apply electric cross fields before and after the ion extraction region (the vertical plates in fig.1). These fields bring the electron beam back to the axis of the apparatus, for analysis in the energy selector and also serve to keep secondary electrons away from the collision region.

3.2. *Measurements of the inelastic scattering of electrons at different angles*. By changing the voltage across the horizontal deflection plates in figure 1, the angle at which the primary beam enters

the collision region may be changed. Thus we can measure in the forward direction electrons scattered through a small angle adjustable from 0 to 5×10^{-2} rad.

For the calibration of the scattering angle, we first adjust the primary beam to pass through the angular selection opening to the decelerating lens. This defines the zero scattering angle. Then we sweep the beam across the opening and record the current on the plate with the opening as a function of the deflecting voltage. From the observed displacement across the opening and the distance to the deflection plates we can calculate the angles corresponding to the applied voltages on the deflection plates. Another calibration point is obtained by repeating this procedure on a second plate with a larger hole and at a shorter distance.

3.3. *Energy loss measurements and the advantages of using a double Wien filter*. When the fast electron beam from the gun collides with the neutral gas beam from the multi-channel gas jet, the electrons will scatter in all directions and will loose different amounts of energy. To detect electrons having lost a certain amount of energy we used an electrostatic magnetic analyzer consisting of a double Wien filter. An electrostatic decelerating lens (see fig.1) is used to decelerate the electrons before entering the energy analyzer. By adjusting the electric and magnetic fields in the filter we allow only electrons with one specific velocity (energy) to pass. Other electrons with different velocities are deflected.

An electron, entering the first filter with velocity v_0 experiences forces in the x- and y- directions (see fig.3), given by:

$$m\ddot{y} = -eF + e\dot{x}B \qquad (1)$$

$$m\ddot{x} = -e\dot{y}B \qquad (2)$$

where F is the electric field strength and B is the magnetic field strength. From equations (1) and (2) one determines[21] the trajectory of this electron (orbit(1) in fig.3) to be:

$$y = A_0 \sin cx + B_0 \cos cx \quad , \qquad (3)$$

where A_0, B_0 and c are constants. This electron passes a paraxial focus for $x = L = \frac{\pi}{c}$.

For another electron with a velocity $v = v_0(1+\beta)$ (where β is small with respect to 1), the trajectory will be[21]:

$$y = A \sin cx + B \cos cx + \frac{\beta}{c} \quad , \tag{4}$$

which is represented by orbit (2) in fig.3. This electron will be focused on the middle diaphragm at a distance:

$$\Delta y_D = \frac{2\beta}{c} = \frac{2\beta L}{\pi} \quad , \tag{5}$$

from the first electron. If we now consider the energy of this electron which is given by:

$$E = E_0(1 + 2\beta) \tag{6}$$

where E_0 is the energy of the first electron and is determined by the deceleration lens voltage, then the energy difference between the two electrons is:

$$\Delta E = E_0 \cdot 2\beta \tag{7}$$
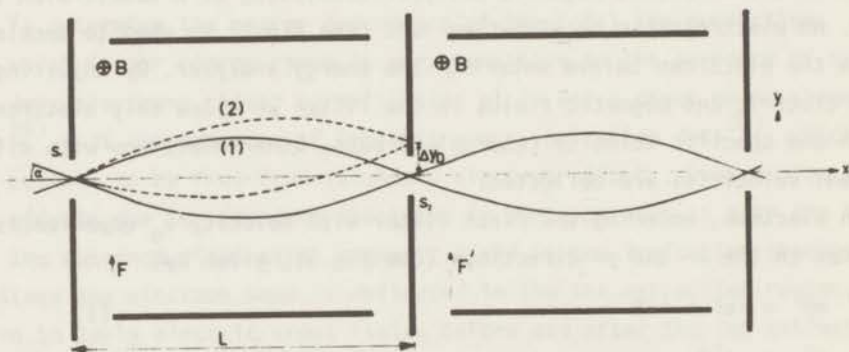
Fig.3. Schematic view of the double Wien filter with electron orbits.

By substituting in equation (5) we get:

$$\Delta y_D = \frac{\Delta E}{E_0} \frac{L}{\pi} \qquad (8)$$

Both electrons will be detected separately if $\Delta y_D \geqslant S_1 + S_2$, where S_1 is the size of the object at the entrance opening and S_2 is the width of the exit slit. Therefore the resolution of the filter is given by:

$$\frac{\Delta E}{E_0} = \frac{\pi (S_1 + S_2)}{L} \qquad (9)$$

Electrons entering the filter with an angle α will suffer an extra displacement[21] $\Delta y_{\alpha 2} = \frac{3\alpha^2 L}{\pi}$ caused by the angular aberration of the filter. For the proper design of the filter for optimum conditions, the displacement due to the dispersion must be in the same order of magnitude as that from the angular aberration, i.e. $\Delta y_D \approx \Delta y_{\alpha 2}$, under this condition the dimensions of the filter can be determined. In our case the entrance opening is an orifice with 0.8 cm diameter and the exit opening is a slit of 0.1×2.0 cm^2. The distance between these openings is 8 cm. The width of the entrance opening is much larger than the width of the object ($\sim 10^{-3}$ cm for $E_0 = 100$ eV) because the exact position of the focus of the decelerating lens is unknown. By changing the decelerating lens voltage between 20 and 100 eV, we obtain an energy spread ΔE of 1 to 5 eV fwhm.

We used a double Wien-filter for the following reasons:

a) When measuring at zero-degree scattering angle, the primary beam enters the filter. Due to reflections from surfaces in the filter the suppression of this beam is never complete. Some of the reflected electrons will reach the detector together with the scattered electrons. This unwanted signal on the electron detector, though it will only increase the number of accidental coincidences, must be kept low. The reason is that in an apparatus with this type of ion extraction, where the target-gas density is necessarily low, typically 10^{-5} torr, the ratio of the number of scattered and primary electrons is very small. At first we used a single filter, where a suppression of the primary beam of $1:10^7$ was obtained. This proved to be insufficient. After using two filters in series this number was improved by a factor of 10^3.

b) Using a single filter, a spread of 25 nsec. in the electron

time-of-flight was obtained for an average electron energy in the
filter of 20 eV. This spread in time-of-flight, which in coincidence
experiment should preferably be kept low, is due to the geometrical
spread of the transmitted electrons over different orbits in the
filter. When introducing a second filter with parallel fields, a
faster-than-average electron from the first filter will, after pas-
sing through the cross-over point at the middle slit, be slower than
average in the second filter. Therefore, the time spread is greatly
reduced.

c) Photons formed in the collision region which might reach the elec-
tron detector are intercepted by placing the middle slit between the
two filters at some distance from the axis of the apparatus. This
does not affect the operation of the filters, since it is possible
to displace the focal point by a proper choice of electric and mag-
netic fields.

The energy selector is always optimized on the elastically scattered
electrons, or on the primary beam when it enters the filter at the
smallest angles. If we then increase the decelerating lens voltage, the
filter transmits inelastically-scattered electrons. The power supplies
are connected such that, when scanning the energy loss, the voltages of
cathode and collision region are all together varied with respect to
the Wien-filter, while the impact energy and the extraction voltage
remain constant. Thus, we keep all voltages between those of the fil-
ters, the electron detector and the surrounding wall, which is on earth
potential, constant in order to ensure a constant over-all detection
efficiency of the electrons.

3.4. *The coincidence data and the automatization.* The number of true
coincidences (n_2-n_1), see section 2.7, represents the relative probabi-
lity for primary electrons to be scattered over a certain angle with a
certain energy loss and producing a certain charge state. The total
number of ions, which arrive at the detector during the accumulation of
the number (n_2-n_1), is a measure for the product of primary beam inten-
sity and target-gas density and may therefore be used to normalize the
coincidence signal. The normal procedure of taking a data run consists
of stepping repeatedly (50 - 100 times) through a range of energy
losses, while the scattering angle and mass spectrometer adjustment are
kept fixed. The number of true coincidences for each energy-loss is

stored in a memory. See ref.22 for more details on the data collection system. An automatization for accumulation of coincidence signals is obtained by making a new step in energy loss (and memory adress) each time a signal integrator, connected to the ion detector, reaches a certain preset value.

4. *Determination of optical oscillator strengths.* In order to obtain data which can be directly compared with those of photo-absorption and photo-ionization experiment, we convert our results on the intensity of electron scattering into optical oscillator strengths. This is possible for such experimental conditions like ours. In our experiment the incident energy of 10 keV is large compared to the energy losses studied ($\leqslant 400$ eV). Also the incident momentum (370 au) is much larger than the momentum transfers ($\leqslant 0.5$ au). Under these conditions the first Born approximation holds, and therefore the differential cross section for scattering of fast electrons can be represented by[23,24] (in au):

$$\sigma(\theta,E) = \frac{2}{E} \frac{k_n}{k_o} \frac{1}{K^2} \frac{df(K)}{dE} \quad , \tag{10}$$

where θ is the scattering angle, E the energy loss, k_o and k_n are the magnitudes of the momenta of the primary electron before and after the collision, K is the magnitude of the momentum transfer ($K = k_o - k_n$) and $(df(K)/dE)$ is the generalized oscillator strength. The generalized oscillator strength may be expanded in terms of K^2:

$$\frac{df(K)}{dE} = \frac{df}{dE} + a K^2 + b K^4 + \ldots \ldots \quad , \tag{11}$$

where $\frac{df}{dE}$ is the optical oscillator strength, as defined in the dipole approximation.

Applying eqs. (10) and (11) to our experiment and taking into account the finite angular resolution of the electron energy analyzer ($\pm 2 \times 10^{-3}$ rad), we may represent the measured intensity of scattering by:

$$I_{scr}(\bar{\theta},E) = \frac{n_c}{n_i} \tag{12}$$

$$\approx \frac{2}{E} \frac{k_n}{k_o} \frac{\int_{\theta_{acc}(\bar{\theta})} (n\ell(\bar{\theta},\theta))_{eff} \, (\frac{1}{K^2} \frac{df}{dE} + a + b K^2 + \ldots \ldots) \, d\theta}{(NL)_{eff} \sigma_i}$$

where $I_{scr}(\bar{\theta},E)$ is the relative intensity of the scattered coincidence signal at an average angle $\bar{\theta}$ (see fig.4) and an energy loss E; n_c is the number of true coincidences; n_i is the total number of ions that is collected on the ion detector while measuring n_c; $\theta_{acc}(\bar{\theta})$ is the range of θ around $\bar{\theta}$ accepted by the analyzer; $(n\ell(\bar{\theta},\theta))_{eff}$ is the effective product of the target-gas density and interaction length for scattering through an angle θ at an average angle $\bar{\theta}$; $(NL)_{eff}$ is the same product for the total production of ions; σ_i is the corresponding ionization cross section. K^2 is the only angular dependent factor in eq. (10).
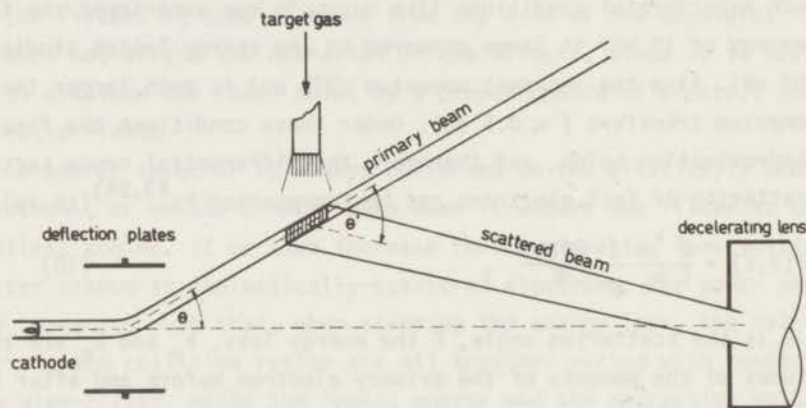
Fig.4. Diagram of collision geometry. θ is the
        deflection angle and $\bar{\theta}$ is the mean scattering
        angle. Ions are extracted from the interaction
        region in a direction perpendicular to the paper.
        The length of this region along the primary beam
        direction is defined by the ion extraction system.

It is given by $k_o^2 + k_n^2 - 2k_o k_n \cos\theta$ and can be approximated by

$$2 E_{el} \{\frac{1}{4} (\frac{E}{E_{el}})^2 + \theta^2\}$$

for our experimental conditions.

Concerning eq. (12) a few remarks must be made:

1. As the over-all detection efficiency of the electron analysis is unknown, we measure a relative $I_{sc}(\bar{\theta},E)$.

2. The part of the electron-beam path which contributes to the scattered coincidence signal, is defined by the ion-extraction system as seen in fig.4.

The distribution of the target-gas density in front of the gas jet is unknown. However, for the small angles that we consider, this unknown distribution over a known length may be replaced by a homogeneous distribution over an effective length. Eventually this length can be varied to evaluate its effect on our calculations and then $n\ell(\bar{\theta},\theta))_{eff}$ may be written as $(NL)_{eff}\, g(\bar{\theta},\theta)$, where $g(\bar{\theta},\theta)$ is a weight function. An approximate weight function $g(\bar{\theta},\theta)$ has been derived from the collision geometry in our apparatus (see ref.25).

Therefore eq. (12) can be reduced to:

$$I_{scr}(\bar{\theta},E) \approx \frac{1}{\sigma_i}\frac{2}{E}\frac{k_n}{k_o}\int_{\theta_{acc}(\bar{\theta})} g(\bar{\theta},\theta)(\frac{1}{K^2}\frac{df}{dE} + a + b\,K^2 + \ldots)d\theta$$

(13)

The term $(NL)_{eff}$ has dropped out. We measure therefore an intensity of scattering relative to the ionization cross section of the product ions that we observe. So by measuring the number of ions we overcome the usual problem of defining the effective-interaction region for near-zero angles, as encountered in typical scattering experiments. Another advantage is that intensities of scattering leading to different charge states of ions may be readily normalized on each other by using the relative abundances of these ions.

The calculated angular dependence of

$$\frac{2}{E}\int_{\theta_{acc}(\bar{\theta})} g(\theta,\bar{\theta})\,\frac{1}{K^2}\,d\theta$$

i.e. the first term in the integral of eq. (13), appears to agree well with the behaviour of $I_{scr}(\bar{\theta},E)$ in our angular range, as measured[25] for a large number of energy losses and various charge states. See for example fig.5. On the basis of this agreement eq.(13) can be simplified to:

$$I_{scr}(\bar{\theta},E) \approx \frac{2}{\sigma_i E}\frac{k_n}{k_o}\frac{df}{dE}\int_{\theta_{acc}(\bar{\theta})} g(\bar{\theta},\theta)\,\frac{1}{K^2}\,d\theta \qquad (14)$$

I_{scatt} (relative)

X E = 25 eV, Ar⁺⁺
I E = 55 eV, Ar⁺⁺
Ô E = 150 eV, Ar⁺⁺
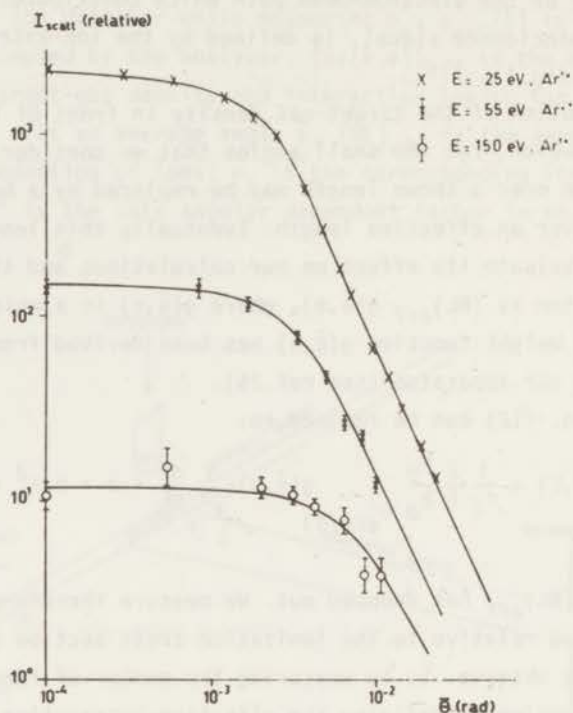
Fig.5.   Plot of relative intensities of scattering against
the average scattering angle at three energy-loss
values. Solid curves: calculated with the integral
in eq.(14).The three series of measurements are on
different relative scales. (Measurements at $\bar{\theta}$ = 0
have been plotted at $\bar{\theta}$ = 10^{-4} rad.

thereby limiting $\bar{\theta}$ to values between 0 and 10^{-2} rad, since outside this
range contributions from optically forbidden transitions, as contained
in the higher terms of eq. (11), will not be negligible. Eq. (14) has
been used to convert our measured $I_{scr}(\bar{\theta},E)$ into relative $\frac{df}{dE}$. However
to obtain absolute values of $\frac{df}{dE}$, a normalization on an absolute value

from photo-absorption or photo-ionization measurements has to be made, using the relation[26] $\frac{df}{dE} = \frac{mc}{\pi e^2 h} \sigma \text{(photoionization)}$.

For the choice of the energy at which we normalize our relative $\frac{df}{dE}$, we require that:

a) a reasonable agreement exists between various authors on the optical value of $\frac{df}{dE}$ at that energy;

b) the energy lies below the lowest threshold for double ionization;

c) no sharp structure is present near this energy within the width of our energy selection;

d) our coincidence signal is high enough to permit an accurate measurement.

REFERENCES

1) Huffman, R.E., Tanaka, Y. and Larrabee, J.C., J.Chem.Phys. 39 (1963) 902.

2) Tanaka, Y. and Takamine, T., Scientific papers of the Institute of Physics and Chemical Research, 39 (1942) 427.

3) Tanaka, Y., Scientific papers of the Institute of Physics and Chemical Research, 39 (1942) 447.

4) De Reilhac, L. and Damany, N., J.de Phys. (1971), to be published.

5) Codling, K. and Madden, R.P., J.Chem.Phys. 42 (1965) 3935.

6) Cairns, R.B., Harrison, H. and Schoen, R.I., Phys.Rev. 183 (1969) 52.

7) Carlson, T.A., Hunt, W.E. and Krause, M.O., Phys.Rev. 151 (1966) 41.

8) Kaneko, T., Omura, I., Yamada, Y. and Tanaka, K., Recent Developments in Mass Spectroscopy, Proceedings of the Int.Conf.on Mass Spectroscopy, University of Tokyo Press, Tokyo (1970) p.751.

9) Al-Joboury, M.I., May, D.P. and Turner, D.W., J.Chem.Soc. (1965) 616.

10) Frost, D.C., McDowell, C.A., Sandhu, J.S. and Vroom, D.A., J.Chem. Phys. 46 (1967) 2008.

11) Siegbahn, K. and co-workers, Atomic molecular and solid state structure studied by means of electron spectroscopy, North-Holland, Amsterdam, 1967 and ESCA applied to free molecules, North-Holland Publ.Comp., Amsterdam, 1969.

12) Mehlhorn, W., Z.Phys. 187 (1965) 21 and 208 (1968) 1.

13) Stalherm, D., Cleff, B., Hillig, H. and Mehlhorn, W., Z.Naturforsch. 24a (1969) 1728.

14) Van der Wiel, M.J., Thesis, University of Amsterdam (1971).

15) Cooper, J.W., Phys.Rev.Letters 13 (1964) 763.

16) Manson, S.T. and Cooper, J.W., Phys.Rev. 165 (1968) 126.

17) Fano, U. and Cooper, J.W., Rev.Mod.Phys. 40 (1968) 441.

18) Van der Wiel, M.J., El-Sherbini, Th.M. and Brion, C.E., Chem.Phys. Lett. 7 (1970) 161.

19) Van der Wiel, M.J., El-Sherbini, Th.M. and Vriens, L., Physica 42 (1969) 411.

20) Schram, B.L., de Heer, F.J., Van der Wiel, M.J. and Kistemaker, J., Physica 31 (1965) 94.

21) Andersen, W.H.J., Een energie analysator voor snelle electronen met hoogscheidend vermogen, afstudeerverslag, T.H.Delft, Delft 1965.

22) Ikelaar, P., Van der Wiel, M.J. and Tebra, W., J.Phys.E (Scientific Instruments) $\underline{4}$ (1971) 102.

23) Bethe, H., Am.Physik $\underline{5}$ (1930) 325.

24) Fano, U., Phys.Rev. $\underline{95}$ (1954) 1198.

25) Van der Wiel, M.J., Physica $\underline{49}$ (1970) 411.

26) Bethe, H. and Salpeter, E.E., Handbuch der Physik, Vol.35, Atoms I. Springer (Berlin, 1957) 334.

CHAPTER II - PART (A)

MULTIPLE IONIZATION OF Kr AND Xe BY 2–14 keV ELECTRONS

TH. M. EL-SHERBINI, M. J. VAN DER WIEL and F. J. DE HEER

FOM-Instituut voor Atoom- en Molecuulfysica, Amsterdam, Nederland

Synopsis

We have measured the relative abundances of multiply charged ions formed by 2–14 keV electrons incident on krypton and xenon. Ion selection is performed in a charge analyzer of 100% transmission. The relative abundances of the multiply charged ions obtained are larger than those given by previous investigators. Partial ionization cross sections are determined by normalization on the absolute ionization cross sections of Schram *et al*. The energy dependence of the partial ionization cross sections is generally in agreement with the Bethe–Born approximation. A good agreement is also obtained between our experimental values for the summation of the proportionality constants of the $E_{el}^{-1} \ln E_{el}$ terms in the cross sections for all the charges and the values calculated by Kingston from photo-absorption data.

1. *Introduction*. Multiple ionization of noble gases has been studied extensively in mass spectrometers[1-4]. Many of these studies have been made at low energies[1,2] (below 600 eV) and a small amount of information is available at high energies. The only data at high energies are those of Fiquet-Fayard[3]) and Stuber[4]) up to 2 keV and of Schram *et al.*[5]) up to 16 keV. The large discrepancies that exist between the results are probably due to discrimination effects[6]) in the ion extraction and detection system, and secondary-electron effects[7]) in the collision region.

In our charge-analyzing system we obtain a transmission[8]) of 100% and consequently we are able to avoid the discrimination effect in the measurement of the relative abundances of the multiply-charged ions (see section 2). Therefore, we may expect our values to be more reliable than those obtained in low transmission mass spectrometers.

The work on Kr and Xe reported here is a continuation of our previous study[8]) of He, Ne and Ar. It presents the experimental relative abundances of the multiply-charged ions formed by 2–14 keV electrons incident on Kr and Xe and the corresponding partial ionization cross sections, obtained after normalization on the absolute gross ionization cross sections of Schram *et al.*

2. *Experimental.* The apparatus has been described in detail in a previous paper [8]. An electron gun produces a beam of electrons which are accelerated to the required energy and collide with the neutral gas atoms emerging from a multi-channel gas jet. A homogeneous extraction field ($\sim$ 100 V/cm) produced by electrodes with large slits (2×1 cm) is used for extraction of the ions. All the ions formed in that part of the collision region which can be seen by the slits are extracted. After analysis in a 30° analyzer magnet the ions are detected by a Bendix M–306 magnetic multiplier connected to a 50 Ω input solid state current amplifier. Detection is performed in the pulse-counting mode; the detection efficiency is independent of the charge of the ions at ion-impact energies above about 4 keV (see ref. 8). The stray magnetic field at the collision region which might cause charge discrimination, was reduced to less than 10^{-2} gauss by shielding [8].

The background pressure is 1×10^{-8} torr. When target gas is introduced, the background pressure rises to about 2×10^{-6} torr and in the collision region we have a few times 10^{-5} torr, as determined from known ionization cross sections [9].

3. *Results and discussion.* 3.1. Multiple ionization cross sections. The multiple ionization cross sections were determined by measuring the relative abundances of multiply-charged ions and normalizing their sum on

TABLE I

E_{el} (keV)	Kr^+ (10^{-17} cm^2)	Kr^{2+} (10^{-18} cm^2)	Kr^{3+} (10^{-18} cm^2)	Kr^{4+} (10^{-18} cm^2)	Kr^{5+} (10^{-19} cm^2)	Kr^{6+} (10^{-19} cm^2)
2	4.30	5.87	4.47	1.32	4.50	1.69
3	3.15	4.60	3.28	1.04	3.18	1.18
4	2.46	3.70	2.74	0.84	2.44	0.89
6	1.81	2.70	1.94	0.56	1.66	0.62
8	1.44	2.18	1.48	0.48	1.31	0.49
10	1.20	1.83	1.29	0.34	0.99	0.41
12	1.03	1.56	1.14	0.30	0.93	0.42
14	0.90	1.41	0.99	0.26	0.89	0.41

E_{el} (keV)	Xe^+ (10^{-17} cm^2)	Xe^{2+} (10^{-17} cm^2)	Xe^{3+} (10^{-18} cm^2)	Xe^{4+} (10^{-18} cm^2)	Xe^{5+} (10^{-18} cm^2)	Xe^{6+} (10^{-19} cm^2)
2	3.68	1.36	8.83	4.41	1.47	7.36
3	2.77	1.03	6.51	3.05	1.04	5.24
4	2.20	0.81	5.28	2.42	0.79	3.96
6	1.65	0.58	3.74	1.79	0.54	2.76
8	1.30	0.47	2.99	1.44	0.38	2.24
10	1.10	0.39	2.42	1.16	0.40	1.93
12	0.96	0.33	2.14	0.97	0.28	1.77
14	0.85	0.29	1.86	0.86	0.26	1.46

Partial ionization cross sections of Kr and Xe

the absolute gross ionization cross sections of Schram *et al.*[7]). At every impact energy we used the absolute values of Schram's gross ionization cross sections in normalizing our relative cross sections for two reasons:

a. They are the only experimental values available from literature in our energy range (2–14 keV).

b. There is a good agreement between his experimental values of $\sum_n M_{nl}^2$ (see section 3.2) for Kr and Xe and the calculated values by Kingston from photo-absorption measurements.

In table I we present our experimental partial-ionization cross sections for 2–14 keV electrons incident on Kr and Xe. Our multiple-ionization cross sections are much higher than Schram's values[7]). This is probably due to a charge-discrimination effect in his mass spectrometer. They are higher by about 24% for 2+ ions up to 68% for 6+ ions.

Figs. 1 and 2 show plots of our experimental values of the relative cross sections for the production of multiply-charged ions of Kr and Xe against the electron-impact energy (2–14 keV). For comparison, the figures also contain the results of Tate and Smith[1]) at small impact energies (up to 600 eV) and those of Stuber[10]) and Schram *et al.*[7]) at high impact energies (up to 14 keV). Stuber's values for the relative abundances of the multiply-charged ions of Kr and Xe were determined from his ionization curves[10])
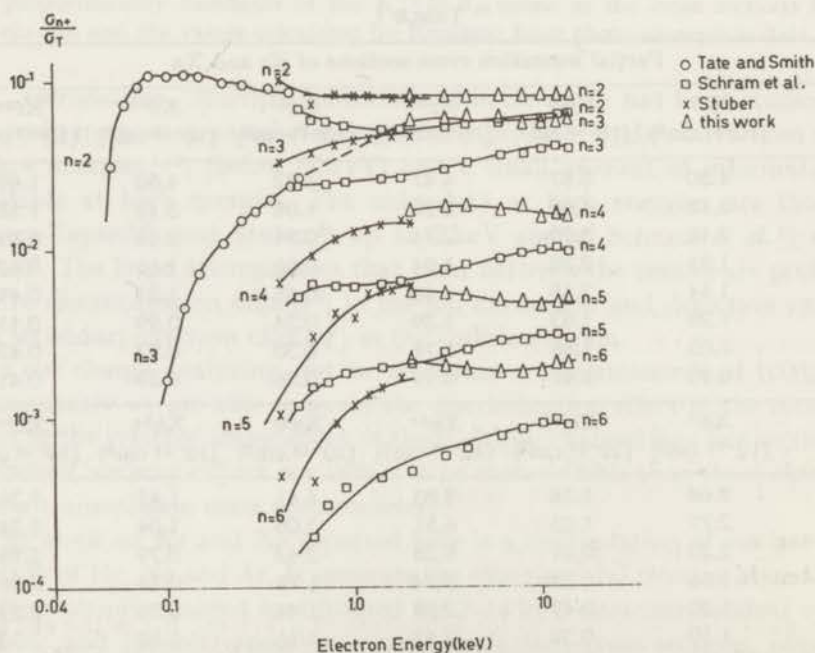
Fig. 1. $\ln(\sigma_{n+}/\sigma_T)$ *vs.* $\ln E_{el}$ for Kr, where σ_{n+} is the cross section for the production of ions of charge $n+$, and σ_T is the total ionization cross section.
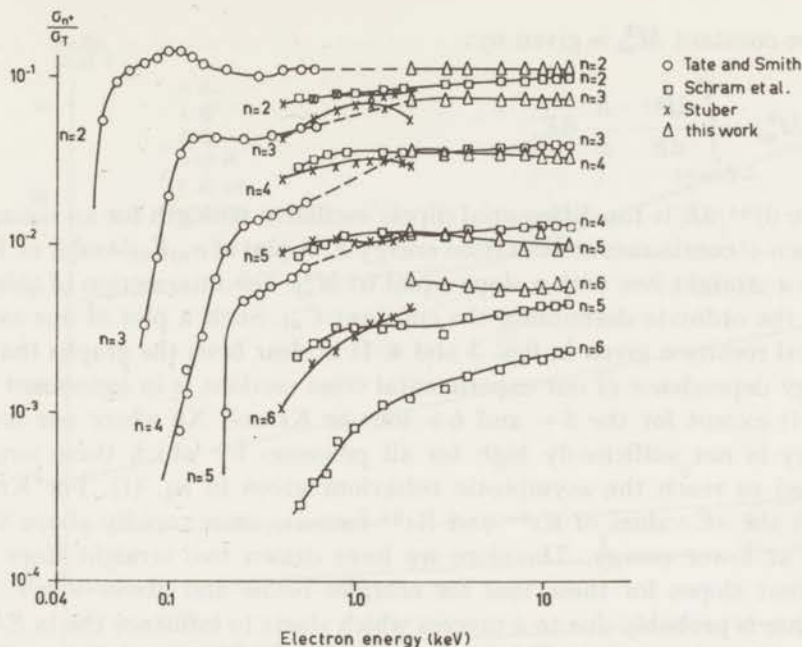
Fig. 2. $\ln(\sigma_{n+}/\sigma_{\mathrm{T}})$ vs. $\ln E_{\mathrm{el}}$ for Xe, where σ_{n+} is the cross section for the production of ions of charge $n+$, and σ_{T} is the total ionization cross section.

and corrected for energy dependence of multiplier efficiency with a method discussed in ref. 7. To obtain the multiple ionization cross sections we normalized the sum of his relative abundances on the absolute gross ionization cross sections of Schram *et al.*[7]). From figs. 1 and 2 it can be seen that our curves appear to fit the curves of Tate and Smith. The values of Schram *et al.* are lower than our values and those of Tate and Smith in the lower energy region. Stuber's values are in general lower than our values at 2000 eV and higher than the values of Tate and Smith at 400 eV. His results are not very accurate because, when changing the focusing properties of the electron gun in his apparatus some variation of the trap current (maximum 10%) between high energy and low energy could not be avoided (see ref. 10).

3.2. Energy dependence of the cross sections. According to the Bethe–Born approximation[11]) the ionization cross section at sufficiently large electron impact energies is given by

$$\frac{\sigma_{ni}E_{el}}{4\pi a_0^2 R} = M_{ni}^2 \ln E_{el} + C_{ni}, \tag{1}$$

where σ_{ni} is the cross section for formation of $n+$ ions, E_{el} is the electron energy, corrected for relativistic effects, a_0 is the first Bohr radius, R is the Rydberg energy and M_{ni}^2 and C_{ni} are constants.

The constant M_{ni}^2 is given by:

$$M_{ni}^2 = \int_{I.P.(n+)}^{\infty} \frac{df^{n+}}{dE} \frac{R}{E}\, dE,$$

where df^{n+}/dE is the differential dipole oscillator strength for an ionization to the $n+$ continuum at excitation energy E. A plot of $\sigma_{ni}E_{el}/4\pi a_0^2 R$ vs. $\ln E_{el}$ gives a straight line with a slope equal to M_{ni}^2. The intersection of this line with the ordinate determines the constant C_{ni}. Such a plot of our experimental results is given in figs. 3 and 4. It is clear from the graphs that the energy dependence of our experimental cross sections is in agreement with eq. (1) except for the 5+ and 6+ ions or Kr and Xe where our impact energy is not sufficiently high for all processes by which these ions are formed to reach the asymptotic behaviour given in eq. (1). For Kr (see fig. 3) the σE values of Kr^{5+} and Kr^{6+} increase more rapidly above 9 keV than at lower energy. Therefore we have drawn two straight lines with different slopes for these ions for energies below and above 9 keV. This increase is probably due to a process which starts to influence the $\ln E$-term in eq. (1) at about 9 keV. This is an L-shell electron ejection (I.P. $L_I = 1.904$, $L_{II} = 1.726$, $L_{III} = 1.675$ keV). An increase was also observed in the graphs
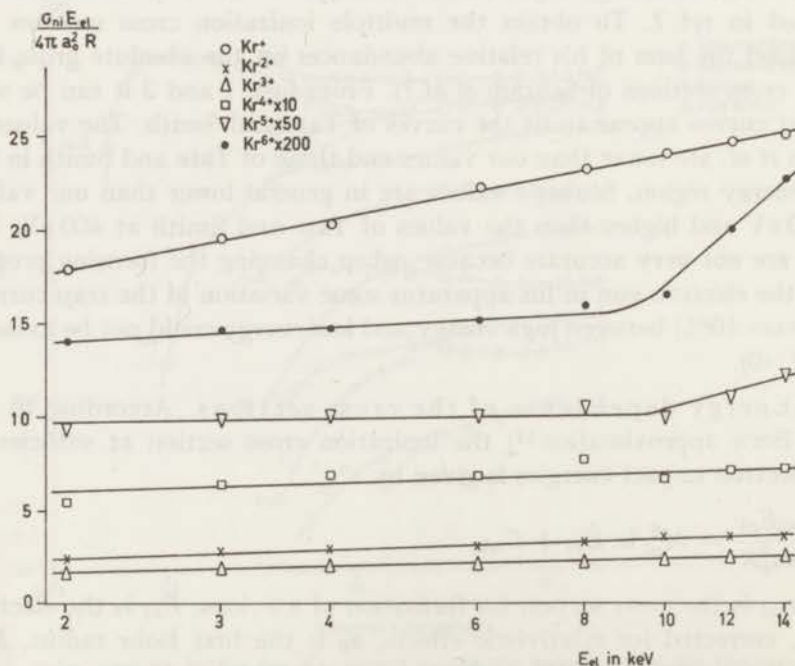
Fig. 3. $\sigma_{ni}E_{el}/4\pi a_0^2 R$ vs. $\ln E_{el}$ for the partial ionization cross sections of Kr.
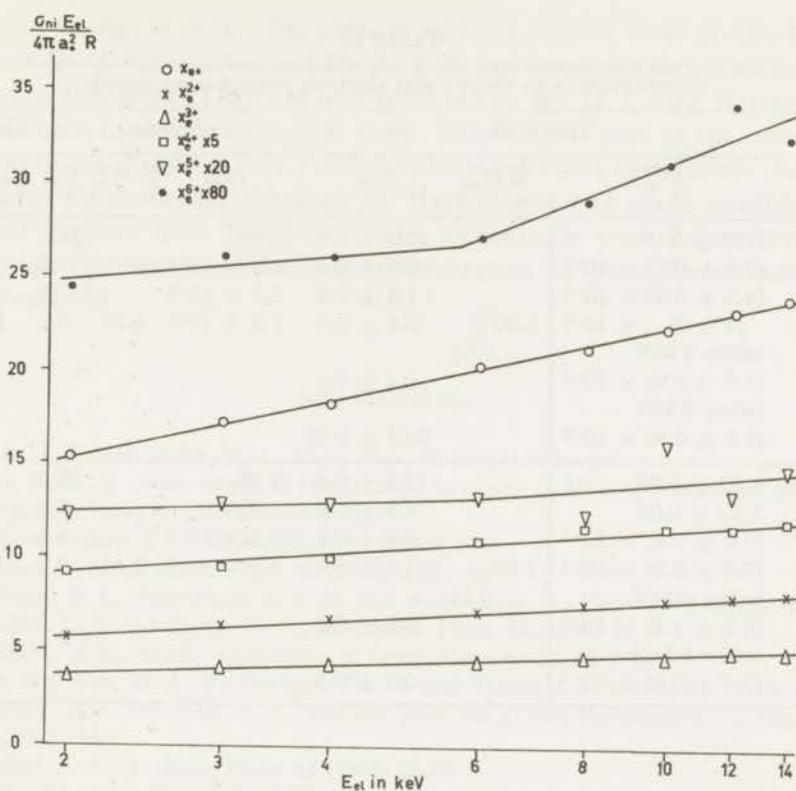
Fig. 4. $\sigma_{ni}E_{el}/4\pi a_0^2 R$ vs. $\ln E_{el}$ for the partial ionization cross sections of Xe.

of Xe^{5+} and Xe^{6+} (see fig. 4) above 6 keV. Two straight lines with different slopes were drawn for each ion, and this increase is probably due to an M-shell electron ejection (I.P. $M_I = 1.15$, $M_{II} = 1.00$, $M_{III} = 0.941$, $M_{IV, V} = 0.67$ keV), that starts to influence the $\ln E$ term at about 6 keV. No increase due to L-shell ionization of Xe (I.P. $L_I = 5.453$, $L_{II} = 5.101$, $L_{III} = 4.782$ keV) is observed since the contribution due to this ionization is small in our energy range. The K-shell ionization potentials of Kr and Xe (I.P. Kr $= 14.324$, Xe $= 34.588$ keV) are above our energy range.

The values of M_{ni}^2 and C_{ni}, obtained by a least-squares analysis of our data, are listed in table II together with the values of Schram[12] for comparison. The table also contains a summation of M_{ni}^2 over the differently charged ions of Kr and Xe ($\sum_n M_{ni}^2$) compared with values given by Kingston[13, 14]. He calculated the continuous oscillator strength from the photo-absorption cross sections. But because the photo-absorption cross sections[15, 16] of Kr and Xe have not been measured accurately in the far ultra-violet and X-ray regions, he adjusted the experimental oscillator strengths such that they produce the experimental refractive index and Verdet constant data[17].

TABLE II

Comparison with theory and electron impact experiments

Ion	This work			Schram			Kingston
	M_{ni}^2	$\sum_n M_{ni}^2$	C_{ni}	M_{ni}^2	$\sum_n M_{ni}^2$	C_{ni}	$\sum_n M_{ni}^2$
Kr^+	3.95 ± 0.08		15.2 ± 0.8	3.95		21.6	
Kr^{2+}	$(7.6 \pm 0.2) \times 10^{-1}$		2.0 ± 0.4	6.6×10^{-1}		1.2	
Kr^{3+}	$(4.8 \pm 0.3) \times 10^{-1}$		1.5 ± 0.5	5.5×10^{-1}		0.5	
Kr^{4+}	$(9 \pm 2) \times 10^{-2}$ below 9 keV	5.30 ± 0.09	0.5 ± 0.4	1.3×10^{-1}	5.29	0.1	5.51
Kr^{5+}	$(1.5 \pm 0.4) \times 10^{-2}$ below 9 keV		0.2 ± 0.1				
Kr^{6+}	$(5.5 \pm 0.9) \times 10^{-3}$		0.07 ± 0.05				
Xe^+	4.50 ± 0.09		12.1 ± 0.8	5.25		28.2	
Xe^{2+}	1.30 ± 0.04		4.9 ± 0.5	1.45		3.3	
Xe^{3+}	$(8.0 \pm 0.4) \times 10^{-1}$		3.2 ± 0.5	5.5×10^{-1}		1.5	
Xe^{4+}	$(3.3 \pm 0.3) \times 10^{-1}$ below 6 keV	7.00 ± 0.11	1.6 ± 0.4	1.9×10^{-1}	7.44	0.5	7.09
Xe^{5+}	$(4.5 \pm 1.2) \times 10^{-2}$ below 6 keV		0.6 ± 0.2				
Xe^{6+}	$(2.9 \pm 0.6) \times 10^{-2}$		0.3 ± 0.1				

From the adjusted sets of oscillator strengths he obtained the values listed in the last column of table II. There is a good agreement between our results and his calculations.

In our previous study[8] on multiple ionization of He, Ne and Ar we made an attempt to evaluate separately two contributions to M_{ni}^2 (for Ne and Ar), namely the one-electron ejection from an inner shell and direct multiple electron ejection from outer shell. This procedure is reasonably justified by the weak interaction between inner and outer shells which is demonstrated by the relatively long Auger lifetimes and the sharpness of the photo-ionization thresholds. However, a recent experiment[18] in which electrons scattered by Ar were detected in coincidence with the ions formed, has shown that M_{2i}^2 and M_{3i}^2 of Ar contain a contribution of 10–15% from simultaneous processes in L and M shells. For Kr and Xe, because of the larger number of electrons in the outer shells, such interaction between inner and outer shells may be stronger than in Ar, which is demonstrated, for instance, by the relatively short $M_{4,5}NN$-Auger lifetime in Kr[19] ($\approx 4 \times 10^{-15}$ s). Therefore, to obtain more detailed information about the contributions due to the processes in the different shells of Kr and Xe, coincidence measurements are necessary.

REFERENCES

1) Tate, J. T. and Smith, P. T., Phys. Rev. **46** (1934) 773.
2) Fox, R. E., J. chem. Phys. **33** (1960) 200; Advances in Mass spectrometry Vol. I, Pergamon Press (London, 1959) p. 397.
3) Fiquet-Fayard, F., J. Chim. phys. **62** (1965) 1065.
4) Stuber, F. A., J. chem. Phys. **42** (1965) 328.
5) Schram, B. L., Boerboom, A. J. H. and Kistemaker, J., Physica **32** (1966) 185.
6) Kieffer, L. J. and Dunn, G. H., Rev. mod. Phys. **38** (1966) 1.
7) Schram, B. L., Thesis, University of Amsterdam, p. 38, 65 (1966).
8) Van der Wiel, M. J., El-Sherbini, Th. M. and Vriens, L., Physica **42** (1969) 411.
9) Schram, B. L., de Heer, F. J., van der Wiel, M. J. and Kistemaker, J., Physica **31** (1965) 94.
10) Stuber, F. A., J. chem. Phys. **42** (1965) 2639.
11) Bethe, H., Ann. Physik **5** (1930) 325.
12) Schram, B. L., Physica **32** (1966) 197.
13) Kingston, A. E., Proc. Phys. Soc. **86** (1965) 467.
14) Kingston, A. E., Schram, B. L. and de Heer, F. J., Proc. Phys. Soc. **86** (1965) 1374.
15) Huffman, R. E., Tanaka, Y. and Larrabee, J. C., J. chem. Phys. **39** (1963) 902.
16) Samson, J. A. R., Phys. Rev. **132** (1963) 2122.
17) Van Vleck, J. H., The Theory of Electric and Magnetic Susceptibilities Clarendon Press (Oxford, England, 1932).
18) Van der Wiel, M. J., to be published in Physica.
19) Nova Acta Regiae Societatis Scientiarum Upsaliensis, Ser. IV. Vol 20, Uppsala 1967.

CHAPTER II - PART (B)

OSCILLATOR STRENGTHS FOR MULTIPLE IONIZATION IN THE
OUTER AND FIRST INNER SHELLS OF Kr AND Xe[*]

Th.M. El-Sherbini and M.J. van der Wiel

Synopsis

Oscillator-strength spectra are reported for the formation of the
charge states one to four following N- and M ionization in Kr and O-
and N ionization in Xe. The spectra were derived from coincidence mea-
surements of small-angle inelastically scattered 10 keV electrons in
the two gases and the ions formed. The spectra of Kr^{1+} and Xe^{1+} put in-
to evidence the presence of a minimum and subsequent maximum in the
contribution of 4p-ϵd transitions in Kr and 5p-ϵd transitions in Xe.
Our study further shows that simultaneous ionization in inner- and
outer shell of the type (3d,N) in Kr and (4d,O) in Xe behaves like a
direct electron interaction process. Its contribution is quite appreci-
able and cannot be neglected when one compares calculated 3d (or 4d)
photoabsorption with experiment. For that purpose we present a number
of separate subshell oscillator-strength distributions. The present
results are compared with photoionization- and absorption data. Their
relation with our previous work on total single and multiple ionization
of Kr and Xe by electron impact is discussed.

1. *Introduction.* It has been shown[1,2] that knowledge of oscillator
strengths for multiple electron transitions is important in the under-
standing of the phenomenon of electron correlation in atoms. On the
one hand, there is direct interaction of the electrons. This has proved
to be responsible for ejection of more than one electron from one

[*] to be published in Physica.

atomic shell. On the other hand, there is the interaction via the
central field, i.e. through changes in the effective nuclear screening.
This is known to be the predominant cause of ejection of outer electrons
subsequent to creation of a deep inner-shell vacancy (electron shake-
off[3]). It is of interest to study systems for which one might expect
the distinction between these two types of interaction to be less sharp
owing to the proximity of the shells involved. Therefore, we now report
a study of multiple electron transitions in the M- and N shell of Kr
and in the N- and O shell of Xe. The strongly collective character of
the electrons in these shells is evidenced by the completely non-hydro-
genic behaviour of the photoabsorption curves[4] of the Kr-M and Xe-N
shells as well as by the shortness of the lifetimes of radiationless
transitions[5] ($\sim 10^{-15}$ sec).

Previous work, both experimental and theoretical, on excitation of
the Kr- and Xe shells mentioned has resulted in data on:
a. The ion charge distribution after irradiation of the two atoms with
   photons at a number of selected wavelengths[6-9];
b. The photoabsorption cross section, experimental[10,13] and theoreti-
   cal[14,16], (i.e. the sum of oscillator strengths of all possible
   transitions) and the high-resolution photoabsorption structure due
   to discrete inner-electron excitations[17] and two-electron excita-
   tions[18];
c. The energies and intensities of electrons emitted in radiationless
   transitions filling inner vacancies[19,20].

The present work is closely connected to that of (a). In our experi-
ment, however, the use of a photon source is simulated by measuring the
small-angle, inelastic scattering of 10 keV electrons in coincidence
with the ions formed. This technique combines the advantage of continu-
ous variability of the energy transfer over a few hundred eV with that
of a constant detection efficiency. As a result oscillator-strength spec-
tra over a wide energy range are obtained, which can be put on an abso-
lute scale by normalization on an absolute photoabsorption value at only
one energy. As far as the intensity is concerned, our method compares
favourably with a possible alternative of charge analysis of ions formed
by dispersed electron synchrotron radiation in a low density target
($\sim 10^{-5}$ torr). Besides, the problem of a wavelength-dependent calibra-
tion of the photon detector is absent in our case.

The results presented here, i.e. oscillator-strength spectra for formation of the charge states one to four in Kr and Xe in a range of energy transfers up to 300 eV, will be discussed in relation with those of the earlier photon- and Auger electron experiments mentioned. We also consider the relation of our previous values[21] on total single and multiple ionization of Kr and Xe by electron impact with the new data on oscillator-strengths.

2. *Experimental*. The apparatus and experimental procedure have been previously described in detail[1,22,23]. Briefly, a 10 keV electron beam passes through a gaseous target of $\sim 10^{-5}$ torr density. The ions produced are extracted and charge analyzed. Electrons scattered through a small angle ($\sim 5 \times 10^{-3}$ rad) are retarded and energy analyzed. Signals from the ion and electron detectors are measured in delayed coincidence. The true coincidences, after being separated from the simultaneously registered accidental ones are stored in a data collector, which drives the energy loss scanning. The number of true coincidences is recorded per number of ions of the charge state under consideration. This enables us to put spectra for different charge states on the same relative scale, when knowing the relative abundances of the charge states at 10 keV electron impact energy. These were determined for Kr and Xe in an earlier study[21].

By making use of the first Born relation for inelastic electron scattering at small momentum transfer, we convert the measured intensities of scattering into oscillator strengths.

As far as background problems are concerned, the Kr^{3+} peak in the mass spectrometer is the only one to coincide with a peak from the background gas (N_2^+). However the contribution of the latter to the mass spectrum of Kr was found to be insignificant.

3. *Results and discussion*.

3.1. General

Oscillator-strength spectra for the formation of the charge states 1+ to 4+ of Kr and Xe via ionization in the outer and the first inner shells are presented in figs. 1-6. Absolute values have been obtained by normalization of our 1+ ion results on the photoionization data of Samson[12] (see figs. 10 and 11) at 30 eV. The spectra were taken

TABLE I

Values of $(df/dE)^{n+}$ for Kr and Xe (n=1 to 4)

Energy loss E (eV)	Kr^{1+} (10^{-2} eV^{-1})	Kr^{2+} (10^{-2} eV^{-1})	Kr^{3+} (10^{-2} eV^{-1})	Kr^{4+} (10^{-3} eV^{-1})	Xe^{1+} (10^{-2} eV^{-1})	Xe^{2+} (10^{-2} eV^{-1})	Xe^{3+} (10^{-2} eV^{-1})	Xe^{4+} (10^{-2} eV^{-1})
20	28.4	-	-	-	23.8	-	-	-
30	14.5	-	-	-	6.70	-	-	-
40	4.2	0.06	-	-	1.60	0.23	-	-
50	1.4	0.12	-	-	0.67	0.40	-	-
60	0.51	0.09	-	-	0.65	0.39	-	-
70	0.43	0.09	-	-	0.71	2.20	0.25	-
80	0.42	0.07	0.02	-	0.93	7.80	2.10	-
90	0.36	0.33	0.04	-	1.19	16.7	5.60	-
100	0.25	0.65	0.21	-	1.14	19.0	8.80	-
110	0.36	1.02	0.35	-	1.75	16.5	8.20	-
120	0.31	1.45	0.64	-	0.71	10.2	5.40	-
130	0.11	1.61	0.95	-	0.10	5.40	2.75	-
140	0.02	2.11	1.22	-	0.26	2.20	1.80	0.05
150	0.16	2.30	1.43	0.04	0.2	0.80	0.80	0.44
160	-	2.42	1.62	0.38	-	0.90	1.25	0.65
170	-	2.37	1.66	0.46	-	0.40	0.51	0.67
180	-	2.60	1.61	0.50	-	0.25	0.10	0.69
190	-	2.50	1.79	0.62	-	0.50	0.75	0.57
200	-	2.54	1.72	0.86	-	0.20	0.10	0.62
210	-	2.82	1.64	1.21	-	-	-	0.61
220	-	2.40	1.90	2.60	-	-	-	0.63
230	-	2.39	2.1	1.21	-	-	-	0.64
240	-	2.15	1.78	1.70	-	-	-	0.53
250	-	2.05	1.91	1.94	-	-	-	0.62
260	-	2.28	1.73	1.75	-	-	-	0.51
270	-	2.00	1.64	2.50	-	-	-	0.42
280	-	2.07	1.75	2.44	-	-	-	-
290	-	1.89	1.24	2.21	-	-	-	-
300	-	1.74	1.61	2.17	-	-	-	-

with an energy resolution of 5 eV fwhm. For Kr^{4+} the scatter in the data points was such that in the figure we show results of a 5-point averaging over the actual points. In table I we have listed the $\frac{df}{dE}$ values at 10 eV energy loss intervals, as obtained from a smooth curve through the data points. The large scatter in the spectra of the single ions at high energy losses is caused by the high number of accidental coincidences counted, when using coincidence time resolutions up to 300 n sec. Such a resolution is necessary owing to the low velocity and consequently large time spread of these heavy ions. The rapidly decreasing intensity of scattering does not permit the use of our method at energy losses beyond the M- and N shell of Kr, or the N- and O shell of Xe. In spite of the small difference in binding energy of the shells mentioned, a first inspection of the spectra shows that it is allowable to divide the discussion into two parts: one concerned with (single and) multiple transitions solely in the outermost shell, and one treating processes which involve an inner electron. In the discussion we shall denote vacancies by writing only those terms of the electron configuration, which have changed with respect to that of the ground state. The ground state of the shells mentioned is given by:

$3s^2 \ 3p^6 \ 3d^{10} \ 4s^2 \ 4p^6$ for Kr and

$4s^2 \ 4p^6 \ 4d^{10} \ 5s^2 \ 5p^6$ for Xe.
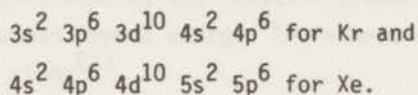
3.2. Ionization in the outer shell

Krypton. The Kr^{1+} spectrum between 20 and 150 eV is shown in fig.1. The region from threshold up to 20 eV has not been plotted, since with an energy resolution of 5 eV fwhm it is not possible to reproduce the known oscillator strengths[12] in the threshold region with any accuracy. The spectrum has the shape of a broad resonance, i.e. it decreases rapidly and passes through a minimum at around 80 eV, the minimum being due to a point of zero in the 4p-ϵd contribution[14] to single ionization. Our Kr^{1+} spectrum gives unambiguous evidence for the presence of such a minimum, since the corresponding maximum at 110 eV is not swamped in the contribution of the 3d shell as is the case in photoabsorption data. Only in the limited range of $3d^9n\ell$ excitation energies some additional single ionization can be expected. Ionization of a 3d electron followed by a radiative transition to a singly ionized state is highly improbable,
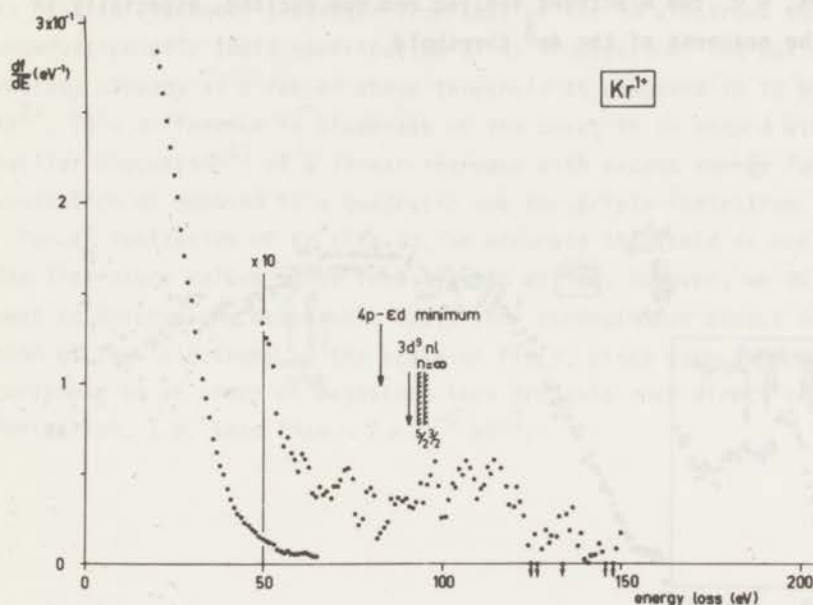
Fig.1. Oscillator-strength spectrum of Kr^{1+}.

while also the spectral shape of $3d^9$ ionization is different from that of the Kr^{1+} maximum (see section 3.3.).

For direct ejection of two N electrons (inset of fig.2,Kr^{2+}), below the $3d^9$ thresholds[19,24], we observe the general features as were found to be characteristic for such transitions[1,2]: a vanishing oscillator strength at the $4p^4$ threshold[24] and a smooth, roughly linear rise to a maximum. The difference with the case of Ar is that the $4p^4$ maximum appears to be reached already at 10 eV above threshold. Thus for ioni-zation to excited Kr^{2+} states, i.e. $4s^1 4p^5$ and $4s^0 4p^6$, a distinctly se-parated second and possibly a third maximum is present. From these se-parate maxima the relative contributions of the various doubly ionized states can be assessed.

A remarkable point about the spectrum is the rise at 75 eV, which cannot be connected with any double transition and which is also too low in energy to be ascribed to discrete excitation of a 3d electron

42

even if allowing for the resolution. We tend to think of triple elec-
tron jumps, e.q. two electrons ionized and one excited, especially in
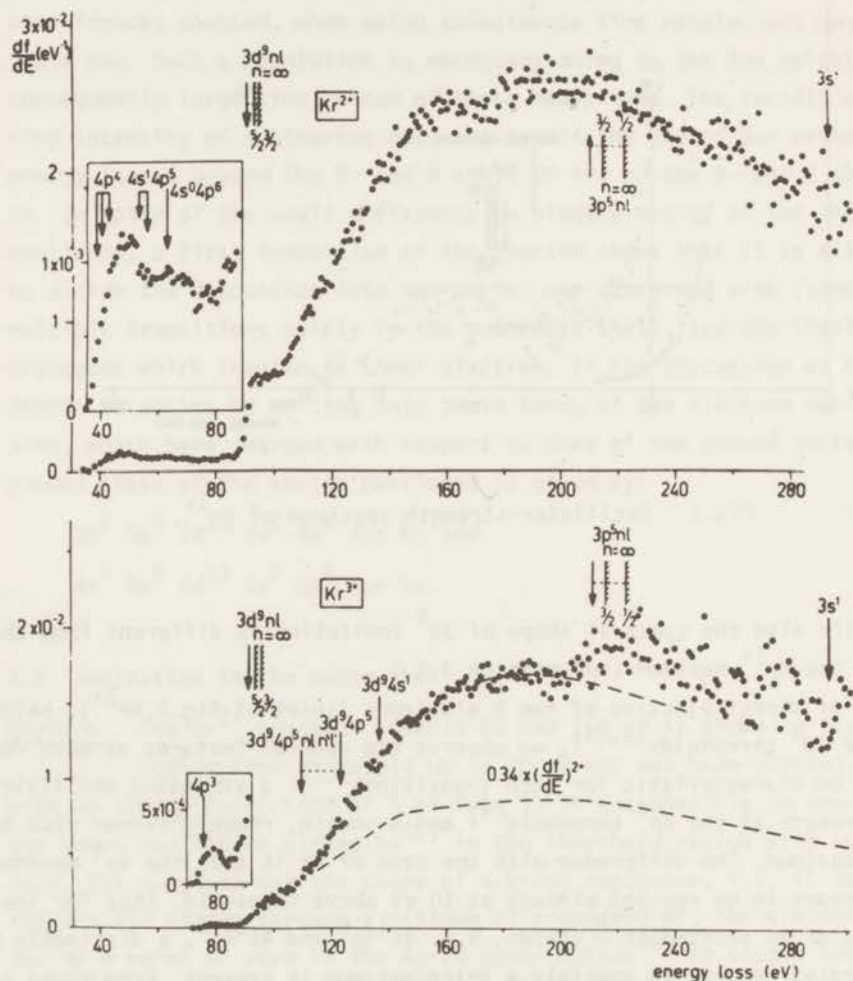view of the nearness of the $4p^3$ threshold.

Fig.2.   Oscillator-strength spectra of Kr^{2+} and
Kr^{3+}.

The threshold for discrete triple ionization[24] (inset of fig.2, Kr^{3+}) is just sufficiently separated from that of the 3d electrons to permit observation of a small contribution of $4p^3$ ionization. The maximum is reached already at a few eV above threshold as compared to 10 eV in Kr^{2+}. This difference in steepness of the onset is in accord with our earlier suggestion[1] of a linear increase with excess energy for double ionization as opposed to a quadratic one for triple ionization.

For 4^+ ionization of Kr (fig.3), an accurate threshold is not known. The literature values range from 118-146 eV [25]. However, we do not expect to observe any measurable oscillator strength for direct ionization of four electrons on the scale of fig.3, since such a process will certainly be an order of magnitude less probable than direct triple ionization, i.e. less than $\sim 2 \times 10^{-5}$ eV^{-1}.
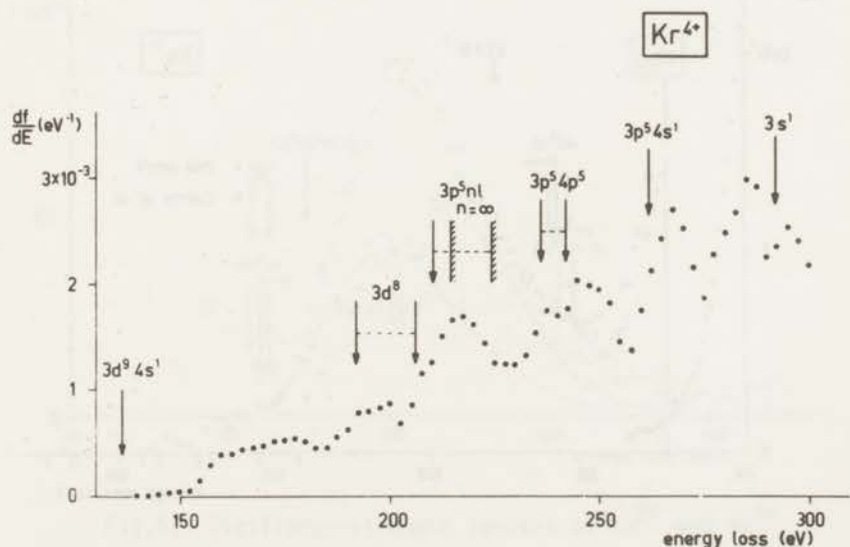

Fig.3.   Oscillator-strength spectrum of Kr^{4+}.
The spectrum has been smoothed by a 5-point
averaging.

<u>Xenon</u>. For Xe^{1+} (fig.4) the situation is quite similar to that for Kr^{1+}. The overall shape of the spectrum is that of a broad resonance with a minimum at about 55 eV, followed by a second maximum at 95 eV. The minimum is presumably due to a point of zero in the 5p-ϵd contribution to single ionization, although no such minimum is present in the 5p subshell contribution as calculated by Manson and Cooper[14]. The bump observed at 47 eV may be due to the maximum in 5s-ϵp ionization, which is predicted at around that energy[14]. A different possibility is the presence of doubly excited states of the type 5s^{1}5p^{5}nℓ n̄ℓ in this energy range. States of this type in the Ar-M shell were found to autoionize either to singly or doubly charged final states[1]. Transitions of 4d electrons to discrete states, i.e. 4d^{9}nℓ, are the only
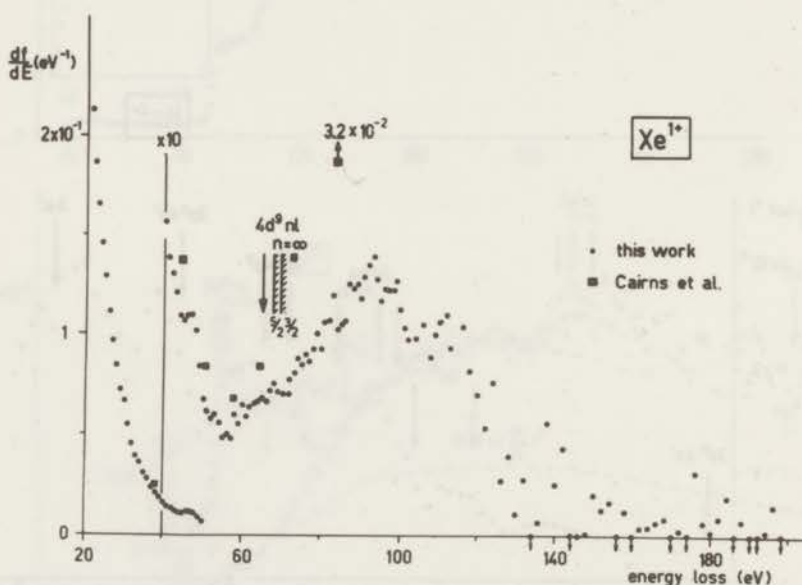
Fig.4. Oscillator-strength spectrum of Xe^{1+}.

inner-shell processes to give rise to Xe^{1+} ions (see section 3.3.). In fig.4 we also plotted a few values obtained by Cairns et al.[8] in a
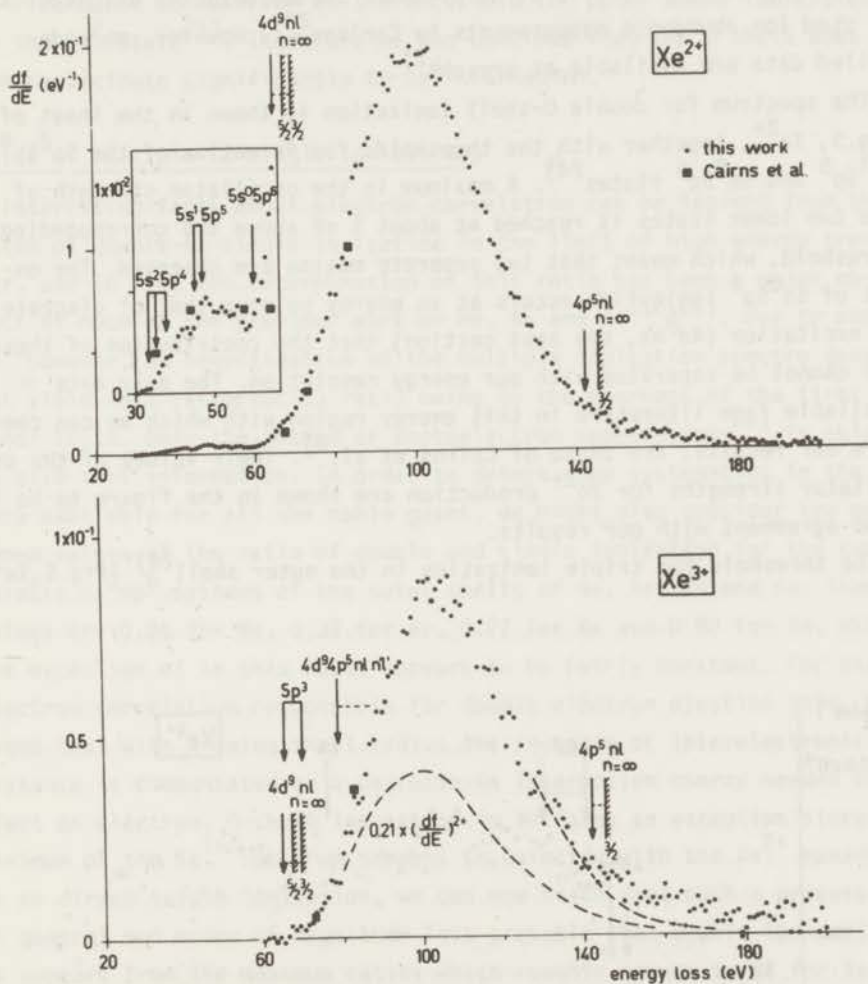
Fig.5. Oscillator-strength spectra of Xe^{2+} and Xe^{3+}.

true photoionization experiment. Their data, which have also been nor-malized on a value of Samson[12] at 28.6 eV, are in good agreement with ours except at the very highest energy transfers. The main source of

discrepancy may be found in the incomplete suppression of low energy
stray photons in the work of ref.8, which is most difficult at the
high energy side of the photon spectrum used. Apart from this, for the
wavelength-dependent calibration of their photon detector Cairns et al.
[8] used ion abundance measurements by Carlson[26]. However, more de-
tailed data are available at present[2].

The spectrum for double O-shell ionization is shown in the inset of
fig.5, Xe^{2+}, together with the thresholds for formation of the $5s^2 5p^4$,
$5s^1 5p^5$ and $5s^0 5p^6$ states[24]. A maximum in the oscillator strength of
the two lower states is reached at about 5 eV above the corresponding
threshold, which means that two separate maxima are observed. The on-
set of $5s^0 5p^6$ ionization occurs at an energy so near that of discrete
4d excitation ($4d^9 n\ell$, see next section) that the contribution of these
two cannot be separated with our energy resolution. The only data
available from literature in this energy region with which we can com-
pare our results, are those of Cairns et al.[8]. Their values of the os-
cillator strengths for Xe^{2+} production are shown in the figure to be in
good agreement with our results.

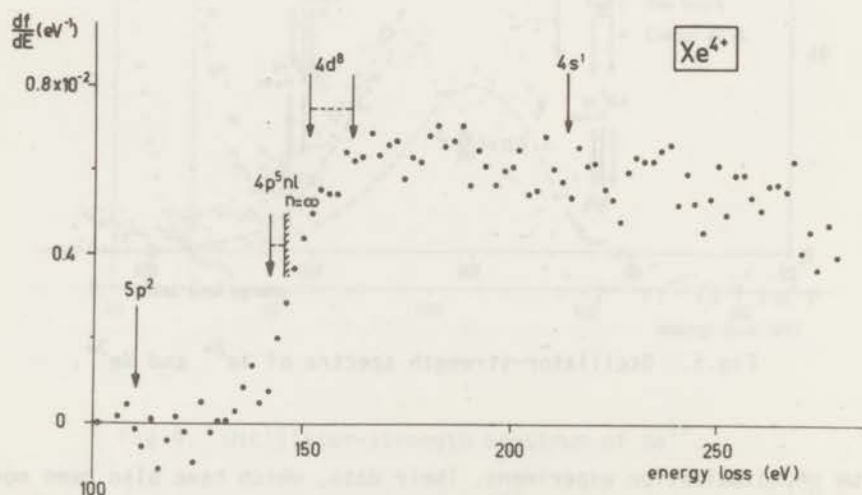The threshold for triple ionization in the outer shell[24] (fig.5,Xe^{3+})

Fig.6. Oscillator-strength spectrum of Xe^{4+}.

almost coincides with that of formation of an inner 4d vacancy. So the occurrence of direct ejection of three electrons cannot be established from an oscillator strength spectrum.

In the case of Xe^{4+} (see fig.6) the situation is rather simple, since no rise could be observed at the threshold for outer shell ionization to the $5p^2$ state[25]. Therefore we can conclude that the O shell does not participate significantly to Xe^{4+} formation.

Ratio of multiple-to-single ionization.

Interesting facts about electron correlation can be learned from the ratio of double-to-single ionization in the limit of high energy trans- fer, and in fact the determination of this ratio has been a major ob- ject of much of the previous work on He, Ne and Ar[1,2,26]. For Kr and Xe, however, an investigation of the multiple ionization spectra does not yield this (asymptotic) ratio owing to the nearness of the first inner shell. Only the method of photoelectron spectroscopy[26] is able to give this information. In order to detect some systematics in the data available for all the noble gases, we might also consider the ma- ximum values of the ratio of double and single ionization for the com- parable ns^2np^6 systems of the outer shells of Ne, Ar, Kr and Xe. These values are 0.26 for Ne, 0.32 for Ar, 0.27 for Kr and 0.80 for Xe. With the exception of Xe this ratio appears to be fairly constant. For the electron correlation responsible for double electron ejection this means that with growing shell radius the increase of interelectronic distance is compensated by a decrease in interaction energy needed to eject an electron. O-shell ionization in Xe forms an exception since the minimum of the Xe^{1+} spectrum happens to coincide with the Xe^{2+} maximum. As to direct triple ionization, we can now state that such a process is in general one order of magnitude less probable than double ionization as appears from the maximum ratios which roughly amount to 2% for Ne, 2% for Ar and 4% for Kr (for Ne and Ar see refs. 1 and 2).

3.3. Ionization in the first inner shell.

In this section we study the ionization following the absorption of energy in the M shell of Kr and the N shell of Xe. In the shells men- tioned, the $3d^{10}$ electrons in Kr and the $4d^{10}$ in Xe are of special inte- rest, since their absorption spectra show the effects of the following

48

phenomena (see ref.4 for a review):

a. The presence of a centrifugal potential barrier for electrons eject-
    ed with high angular momentum, which accounts for the delayed ab-
    sorption maximum for the dominant transition nd-εf. Transitions of
    the type nd-εp, which behave more hydrogen-like, are generally much
    less abundant especially in the case of Xe. Their contribution can
    only be observed in the Kr absorption as a sharp jump at the $3d^9$
    threshold (see fig.2). The jump is followed by a much more extended
    rise to the delayed 3d-εf maximum.

b. A minimum (in Xe) in the contribution of 4d-εf transitions at around
    200 eV [14], which gives rise to a much faster decrease of the 4d ab-
    sorption in Xe (fig.5) after the maximum than in the case of Kr.

c. A collective character of the 3d and 4d electrons in Kr and Xe. A
    single-particle model, when taking into account phenomena (a) and
    (b), predicts an nd absorption which is far higher and more sharply
    peaked[27] than observed experimentally. Much better agreement with
    experiment is obtained when using a plasma-type treatment[15,28].

The various initial vacancies, data on their energies and possible
paths of decay via radiationless transitions, have been listed in
tables II and III and will be discussed following the sequence in the
tables. Radiative transitions will be assumed to contribute to a negli-
geable amount* throughout the discussion. Data on the energies of dis-
crete excited states are from photoabsorption measurements mostly
[17,18,31], while for ionization threshold data from photoelectron and
Auger electron experiments have been used[19,20].

_____

* This is justified by the fluorescence yields known for other
  cases[29,30] and the trend with decreasing Z and increasing
  principal quantum number of the vacancy.

TABLE II

M processes in Kr

Threshold energy (eV)	References	Initial vacancies	Radiationless transition(s) to:*	Ion charge observed
$^2D_{5/2}$:91.4	17	$3d^9n\ell$	→ $4p^5$+e	1+
$^2D_{3/2}$:92.5			→ $4p^4$+2e	2+
$^2D_{5/2}$:93.8	17,20	$3d^9$	$\xrightarrow{75\%}$ $4p^4$+e	2+
$^2D_{3/2}$:95			$\xrightarrow{25}$ $4p^3$+2e	3+
108.9	18	$3d^94p^5n\ell\,\bar{n}\ell$	→ $4p^{6-x}$+xe (mostly x=3)	(1+, 2+) 3+
121.2-123.4	19	$3d^94p^5$	→ $4p^3$+e	3+
135.6-136.8		$3d^94s^1$	→ $4p^2$+2e ?	4+ ?
192.1-207.1	19	$3d^8$	→ $4p^2$+2e	4+
211	31	$3p^5n\ell$	$\xrightarrow{e.g.**}$ $3d^94p^5$+2e→ $4p^3$+3e ↘ $4p^2$+4e	3+ 4+
$^2P_{3/2}$:214.6	19,20,31	$3p^5$	→ $3d^94p^5$+e→ $4p^3$+2e (60%) ↘ $4p^2$+3e	3+
$^2P_{1/2}$:222.1			→ $3d^94p^4$+2e→$4p^2$+3e }(40%) → $3d^8$+e → $4p^2$+3e	4+
235.1-242.1	19	$3p^54p^5$	→ $3d^94p^4$+e→ $4p^2$+2e	4+
264 ?	this work	$3p^54s^1$		
292.5	19,20	$3s^1$	$\xrightarrow{e.g.*}$ $3d^94s^1$+e→ $4p^3$+2e ↘ $4p^2$+3e	3+ 4+

---

* The final transitions to multiply charged states have been denoted for clarity as if depleting only the outer p subshell. Of course in most cases the outer s subshell is involved as well.

** e.g. is used in those cases, which are believed to be the most probable.

<u>Krypton</u>. Excitation of a 3d electron to a discrete state ($3d^9 n\ell$) can
lead to single or double ionization, depending on whether the
excess energy of the subsequent Auger transition is carried away by one
or two electrons. Similar transitions were observed before in L excita-
tion in Ar[1]. For the Kr^{1+} spectrum this means that in the range of
$3d^9 n\ell$ energies (91-95 eV) there is probably some contribution which lo-
cally enhances the rise after the 4p-εd minimum. The decay via double
electron ejection is represented in the Kr^{2+} spectrum as a shift of the
3d-jump to 90 eV, a few eV below the thresholds for $3d^9$ ionization.

After ionization of a 3d electron the most abundant product is Kr^{2+},
the double electron ejection leading to Kr^{3+}. The branching over double
and single electron ejection has a ratio of 0.34 (i.e. 75% Kr^{2+} and 25%
Kr^{3+}, table II), as can be derived from the small plateau value in the
ratio $(\frac{df}{dE})^{3+}/(\frac{df}{dE})^{2+}$ (fig.7) right above the $3d^9$ thresholds. The shape
of the Kr^{2+} spectrum above 90 eV can be considered to be that of a pure
$3d^9$ absorption since all higher processes lead to higher charge states
(see table II). Knowing the fraction with which the $3d^9$ hole configura-
tion contributes to the Kr^{3+} spectrum, i.e. 0.34 $(\frac{df}{dE})^{2+}$, we can ascribe
the remaining oscillator strength to higher processes (see fig.2).

Firstly, simultaneous excitation in M- and N shell ($3d^9 4p^5 n\ell\hat{n}\hat{\ell}$)which
according to the rise in the ratio (fig.7) decays mainly to Kr^{3+}. Second-
ly, simultaneous ionization in M- and N shell ($3d^9 4p^5$ and $3d^9 4s^1$),
which can only lead to Kr^{3+} and possibly in the case of $3d^9 4s^1$, to Kr^{4+}
(fig.3)*.

Double ionization in the M shell corresponding to $3d^8$ states is observ-
ed in Kr^{4+} as a rise at around 200 eV. The onset energies for these
states were obtained in Auger electron spectroscopy[19].

The rise in the Kr^{3+}- and Kr^{4+}-spectrum at 210 eV are due to excita-
tion ($3p^5 n\ell$) and ionization ($3p^5$) of 3p electrons. The most abundant de-
cay, to Kr^{3+}, occurs via a Coster-Kronig transition, the second step
being an Auger transition. Double electron ejection in either of the two
steps leads to Kr^{4+} formation. A one-step Auger decay (→ Kr^{2+}) was re-
ported by Mehlhorn[19] to contribute less than 10% to the decay of a 3p

---

* The energy of the $4p^2$ state is not known accurately (see section
3.2.). The Kr^{4+} spectrum is not sufficiently detailed to draw any
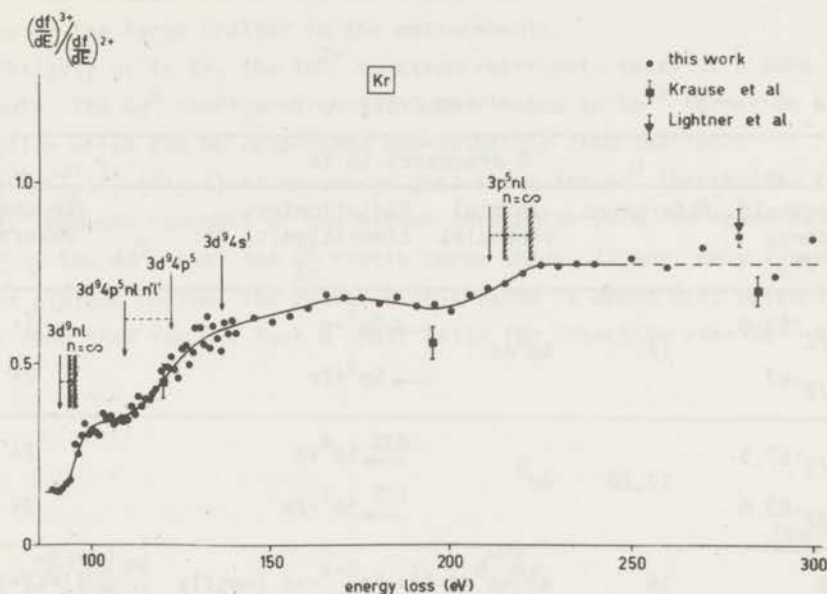conclusions in this respect.

Fig.7. Ratio of oscillator-strengths for triple and
double ionization of Kr; up to 140 eV all data
points are shown; at higher energies only average
ratios over wider intervals are given;
■ —— ref.7; ▼ —— ref.9.

vacancy. Therefore no jump in our Kr^{2+} spectrum is visible. Simultaneous
ejection of a 3p- and an outer electron ($3p^5 4p^5$ and $3p^5 4s^1$) can only
lead to Kr^{4+} formation (see the corresponding jumps in fig.3).

The $3s^1$ vacancy decays to both Kr^{3+} and Kr^{4+}, the most likely process
according to Auger electron spectroscopy[19] being a Coster-Kronig tran-
sition (see table II).

Xenon. In the first instance N processes in Xe (see table III) are si-
milar to those occurring in the M shell of Kr. Therefore in our
discussion of the decay possibilities we shall confine ourselved to
pointing out the differences and similarities with Kr.

TABLE III

			N processes in Xe		
Threshold energy (eV)	References	Initial vacancies	Radiationless transition(s) to:*		Ion charge observed
$^2D_{5/2}$:63.9	17	$4d^9n\ell$	$\longrightarrow 5p^5+e$		1+
$^2D_{3/2}$:67			$\longrightarrow 5p^4+2e$		2+
$^2D_{5/2}$:67.5	17,20	$4d^9$	$\xrightarrow{83\%} 5p^4+e$		2+
$^2D_{3/2}$:69.5			$\xrightarrow{17\%} 5p^3+2e$		3+
77.8	18	$4d^95p^5n\ell$	$\bar{n\ell}\rightarrow 5p^{6-x}+xe$ (mostly x=3)		(1+,2+)3+
		$4d^95p^5$ $4d^95s^1$	$\longrightarrow 5p^3+2e$		3+
142	18	$4p^5n\ell$	$\xrightarrow{e.g.^{**}} 4d^95p^5+2e\rightarrow$	$5p^3+3e$	3+
				$5p^2+4e$	4+
$^2P_{3/2}$:145.5	18,20	$4p^5$	$\longrightarrow 4d^95p^5+e\rightarrow$	$5p^3+2e$ (50%)	3+
				$5p^2+3e$ (50%)	4+
$^2P_{1/2}$:-			$\longrightarrow 4d^95p^4+2e\rightarrow 5p^2+3e$		
151.5-161.8	20	$4d^8$	$\longrightarrow 5p^2+2e$		4+
212.2	20,31	$4s^1$			

* The final transitions to multiply charged states have been denoted for clarity as if depleting only the outer p subshell. Of course in most cases the outer s subshell is involved as well.

** e.g. is used in those cases, which are believed to be the most probable.

The decay of $4d^9 n\ell$ states in Xe is visible as small bump in the Xe^{1+} curve which adds up to the rise after the $5p-\varepsilon d$ minimum. Such a bump could not be observed for the corresponding states in the Kr^{1+} curve because of the large scatter in the measurements.

Similarly as in Kr, the Xe^{2+} spectrum represents decay of a pure $4d^9$ vacancy. The $4d^9$ configuration also contributes to Xe^{3+} formation with a fraction which can be determined approximately from the ratio $(\frac{df}{dE})^{3+}/(\frac{df}{dE})^{2+}$ (fig.8) at an energy just above the $4d^9$ thresholds. It is clear from the nearness of the higher thresholds (e.g. $4d^9 4p^5 n\ell \; \bar{n}\bar{\ell}$) to that of the $4d^9$, that the $\frac{3+}{2+}$ -ratio curve shows, if any, only a very short plateau region. The ratio in this range is about 0.21 which is less than that for Kr. Such a small ratio for branching over Xe^{3+} and
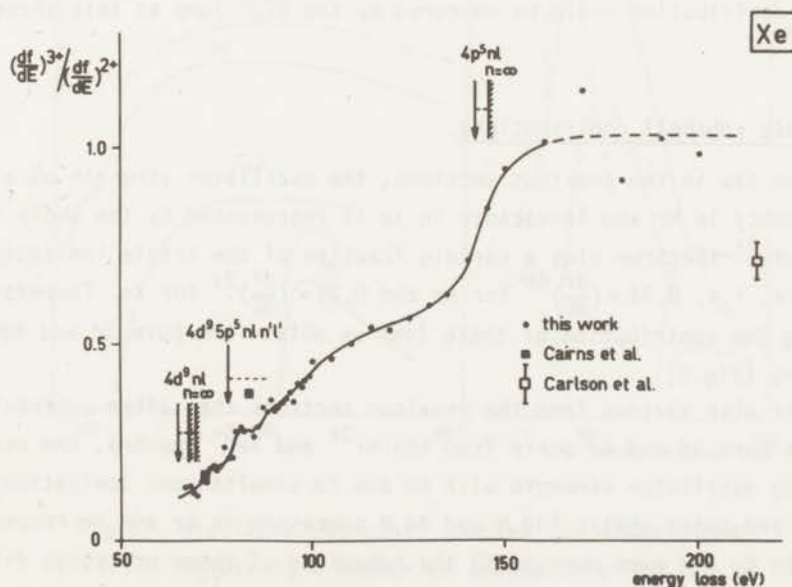

Fig.8. Ratio of oscillator-strengths for triple and double ionization of Xe; up to 100 eV all data points are shown; at higher energies only average ratios over wider intervals are given;
■ —— ref.8; □ —— ref.6.

Xe^{2+} is expected, since in the decay of the $4d^9$ vacancy to Xe^{3+} only one or two of the lowest configurations ($5p^3$ levels) of this ion are accessible while decay to any of the excited configurations is energetically impossible (see fig.5, Xe^{3+}).

The thresholds for simultaneous ionization in the N- and O shell ($4d^95p^5$ and $4d^94s^1$) are not known from Auger electron spectroscopy. However, the contribution of these initial vacancy states is clear, when we subtract the pure $4d^9$ contribution ($0.21 \times (\frac{df}{dE})^{2+}$) from the Xe^{3+} spectrum.

The large jump in the Xe^{4+} spectrum at the $4p^5$ threshold indicates a predominant contribution to the formation of this ion. Structure due to higher thresholds is not observed (see fig.6).

A possible contribution of $4d^8$ states to the Xe^{4+} spectrum similar to that of $3d^8$ states of Kr is expected though no clear structure is observed at the onset energies for these states. This is because in the case of Xe they lie just above the $4p^5$ threshold (see fig.6) where their contribution could be obscured by the high jump at this threshold.

Separate subshell contributions.

As we saw in the previous sections, the oscillator strength of a pure 3d-vacancy in Kr and 4d-vacancy in Xe is represented by the whole Kr^{2+} resp. Xe^{2+}-spectrum plus a certain fraction of the triple ionization spectra, i.e. $0.34 \times (\frac{df}{dE})^{2+}$ for Kr and $0.21 \times (\frac{df}{dE})^{2+}$ for Xe. Therefore by adding the contribution of these ions we obtain the pure 3d and 4d-spectra (fig.9).

It is also obvious from the previous sections that after subtraction of the pure 3d and 4d-parts from the Kr^{3+} and Xe^{3+} spectra, the remaining oscillator strength will be due to simultaneous ionization in inner and outer shells (3d,N and 4d,O processes in Kr and Xe respectively). In Kr and even more in Xe the behaviour of these processes differs from that of corresponding 2p,M transitions in Ar[1], where the process had all characteristics of electron shake-off, i.e. a sharp jump in branching ratio at threshold followed immediately by a plateau value. The (3d,N) ionization in Kr and the (4d,O) in Xe, however, makes the $\frac{3+}{2+}$ ratio rise over an extended range above threshold and pass through a maximum for Kr. This behaviour is more like the one characteristic for

direct electron interaction which is not surprising for two shells
which have only $\sim$ 80 eV energy separation in Kr and $\sim$ 50 eV in Xe. The
oscillator-strength spectra derived for (3d,N) and (4d,0) transitions
are shown in fig.9.

Finally the spectra for 3p ejection in Kr and 4p ejection in Xe can
be estimated roughly. We do this by extrapolating the (3d,N) and (4d,0)
contributions in the Kr^{3+} and Xe^{3+} curves across the $3p^5$- and $4p^5$
thresholds (see dashed lines in figs. 2 and 5) and evaluating the $3p^5$
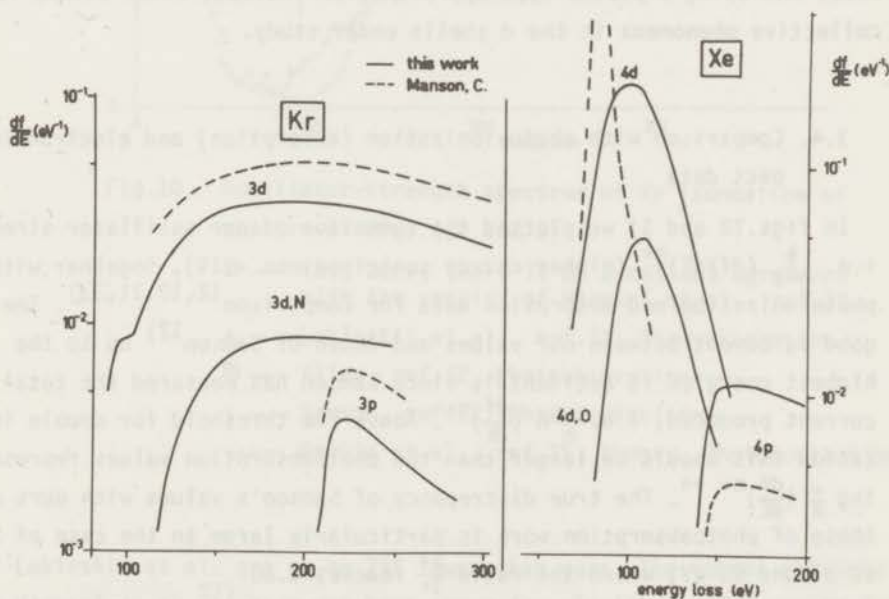and $4p^5$-contributions. We then add these to the estimated $3p^5$ and $4p^5$-

Fig.9. Oscillator-strength spectra for transitions
involving a number of subshells of Kr and Xe
Solid curves - this work;
Dashed curves - Manson and Cooper, ref.14.

Kr^{4+} and Xe^{4+}-spectra and obtain the spectra given in fig.9.

At the $3p^5$ threshold of Kr and the $4p^5$ threshold of Xe, an increase
is observed in the $\frac{3+}{2+}$ -ratio curves (figs.7 and 8). After this increase
a constant branching ratio of 0.75 for Kr and 1.0 for Xe is reached.

Further changes are not expected, since higher processes only produce higher charge states. In the figures we also plotted all data in literature with which we can compare our results. The discrepancy between our results and those of Carlson et al.[6] for Xe is unsatisfactory. The reason for this large discrepancy is not known.

We also plotted the theoretical results for the various subshells by Manson and Cooper[14], who used a single-particle model*. The discrepancies of their data and ours are generally large (One has to keep in mind that our 3p and 4p spectra are not more than rough estimates). In the following section we shall see that most of the large discrepancy for the d-electrons can be removed by discarding the single-particle model and using a plasma type approximation instead, which allows for collective phenomena in the d shells under study.

3.4. Comparison with photo-ionization (absorption) and electron impact data

In figs.10 and 11 we plotted the summation of our oscillator strengths, i.e. $\sum_{n=1}^{4} (df/dE)^{n+}$ (higher charge contributions < 1%), together with photoionization and absorption data for comparison[12,10,11,33]. The good agreement between our values and those of Samson[12] up to the highest energies is accidental, since Samson has measured the total ion current produced, i.e. $\sum_{n} n (\frac{df}{dE})^{n+}$. Above the threshold for double ionization this should be larger than the photoabsorption values representing $\sum_{n} (\frac{df}{dE})^{n+}$ **. The true discrepancy of Samson's values with ours and those of photoabsorption work is particularly large in the case of Xe at around 60 eV, where the ratio $\frac{2+}{1+}$ reaches 0.80.

The agreement of the present results with that of the other experiments is quite satisfactory, except in the case of Kr, where the data

---

* With a similar model McGuire[32] calculated the 3d-εf cross sections of Kr and the 4d-εf cross sections of Xe, and obtained excellent agreement with the data of Manson and Cooper.

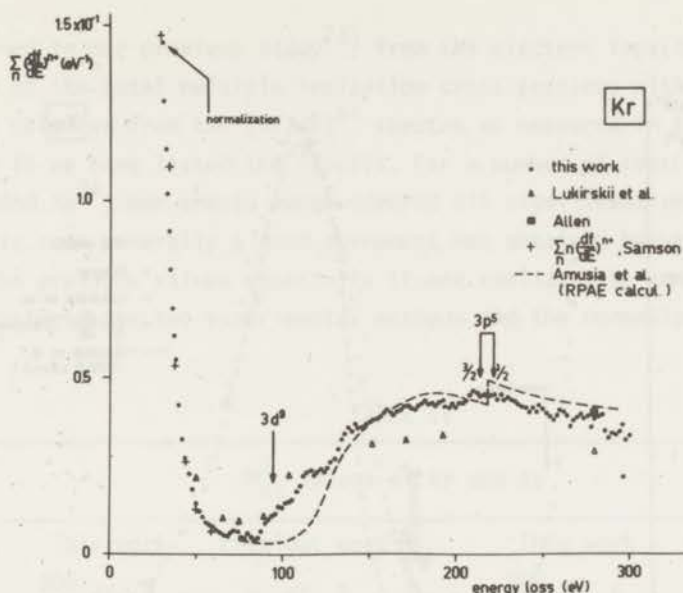** This point was not recognized in the paper by Cairns et al.[8].

Fig.10. Oscillator-strength spectrum of Kr (summation of
spactra of figs.1,2 and 3);

●—— this work; there is an excellent agreement
with the results of Haensel et al., ref.13.

Δ —— Lukirskii et al., ref.10, Photoabsorption.

■ —— Allen, ref.32, Photoabsorption.

+ —— Samson, ref.12, Photoionization.

----- Amusia et al., ref.15, theory, Photoionization.

of Lukirskii et al. are up to 25% lower than ours. The curves obtained
by Haensel et al.[13] have not been shown for clarity; their results for
Kr almost coincide with our results, while for Xe their results are
identical to those of Ederer[11]. Figs.10 and 11 also contain the theo-
retical 3d- and 4d spectra of Amusia et al.[15], calculated in a plasma-
type model, the random phase approximation with exchange (Recently for
Xe a similar result was obtained by Wendin[28]). It is evident that this
model is far superior to the single-particle model. Only close to thres-
hold some discrepancy is left. In this context we might comment on the
care that has to be excercised in comparing calculated and measured
curves for the cases under consideration. In the first place the two
outer p sub-shells produce a maximum (see Kr^{1+} and Xe^{1+}) in the range
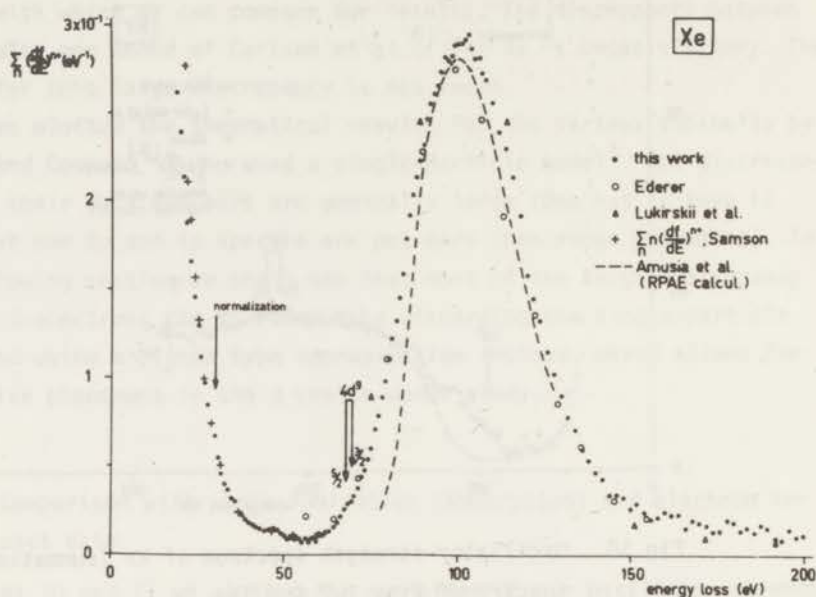
Fig.11. Oscillator-strength spectrum of Xe (summation of spectra of figs.4,5 and 6);

● —— this work;

○ —— Ederer, ref.11, Photoabsorption; these points agree closely with the results of Haensel et al., ref.13;

Δ —— Lukirskii et al., ref.10, Photoabsorption;

+ —— Samson, ref.12, Photoionization;

----- Amusia et al., ref.15, theory, photoionization.

of comparison. In the second place a quite substantial fraction of the total absorption has been shown to arise from simultaneous inner- and outer shell transitions (see fig.9) which are generally not included in the calculations.

It is interesting to compare the values of $M^2_{ni} = \int_{I.P.^{n+}}^{\infty} (df/dE)^{n+} \frac{R}{E} dE$ (R is Rydberg energy),

obtained in our previous study[21] from the electron impact energy dependence of the total multiple ionization cross sections with similar integrals obtained from the $(df/dE)^{n+}$ spectra as measured in this work. In table IV we have listed the results. For a number of ions(Kr^{1+}, Xe^{1+}, Xe^{2+} and Xe^{3+}) our energy range covered all significant energy transfers. In this case generally a good agreement was obtained between the present and the previous values especially if one realizes the complete difference between the two experimental methods and the normalization, which

TABLE IV

M^2_{ni}-values of Kr and Xe

Ion	This work $\int_{I.P.}^{300}(\frac{df}{dE})\frac{R}{E}dE$	Previous work[21] $\int_{I.P.}^{\infty}(\frac{df}{dE})\frac{R}{E}dE$	Ion	This work $\int_{I.P.}^{200}(\frac{df}{dE})\frac{R}{E}dE$	Previous work[21] $\int_{I.P.}^{\infty}(\frac{df}{dE})\frac{R}{E}dE$
Kr^{1+}	3.92±0.15	3.95±0.08	Xe^{1+}	3.90±0.2	4.5±0.09
Kr^{2+}	3.4×10^{-1}	$(7.6±0.2)\times10^{-1}$	Xe^{2+}	1.15±0.1	1.3±0.04
Kr^{3+}	2.0×10^{-1}	$(4.8±0.3)\times10^{-1}$	Xe^{3+}	$(5.2±0.7)\times10^{-1}$	$(8.0±0.4)\times10^{-1}$
Kr^{4+}	1.1×10^{-2}	$(9 ±2)\times10^{-2}$	Xe^{4+}	6.4×10^{-2}	$(3.3±0.3)\times10^{-1}$

is on photoionization cross sections in this work and on total electron cross sections in ref.21. For the other ions the present measurements do not extend to sufficiently high energies to measure M^2_{ni} completely.

4. *Conclusion.* From coincidence measurements of the small-angle inelastically scattered electrons in Kr and Xe and the ions formed we were able to demonstrate the presence of a minimum followed by a maximum in the contribution of 4p-εd transitions in Kr and 5p-εd transitions in Xe. These minima and maxima are obscured in the photoabsorption measurements by the rapidly rising contributions of 3d and 4d transitions in Kr and Xe respectively. Furthermore our results showed the existence of strong direct interaction between electrons in the outer- and inner shells, as opposed to a "shake-off" type-interaction in Ar. This puts into evidence the importance of the correlation between these

shells of Kr and Xe which is not considered in most of the calculations and is at least partly responsible for the discrepancies which exist between the experimental results of the oscillator strengths and those predicted by theory.

Acknowledgements

REFERENCES

1. Van der Wiel, M.J. and Wiebes, G., Physica 53 (1971) 225.
2. Van der Wiel, M.J. and Wiebes, G., Physica 54 (1971) 411.
3. Carlson, T.A., Nestor, C.W., Tucker, T.C. and Malik, F.B., Phys. Rev. 169 (1968) 27.
4. Fano, U. and Cooper, J.W., Rev. Mod. Phys. 40 (1968) 441.
5. Nova Acta Regiae Societatis Scientiarum Upsaliensis, Ser.IV. Vol. 20, Uppsala 1967.
6. Carlson, T.A., Hunt, W.E. and Krause, M.O., Phys.Rev. 151 (1966) 41.
7. Krause, M.O. and Carlson, T.A., Phys.Rev. 158 (1967) 18.
8. Cairns, R.B., Harrison, H. and Schoen, R.I., Phys.Rev. 183 (1969) 52.
9. Lightner, G.S., Van Brunt, R.S. and Whitehead, W.D., Phys.Rev. 4 (1971) 602.
10. Lukirskii, A.P., Brytov, I.A. and Zimkina, T.M., Opt.Spectrosc. (USSR)(English Translation) 17 (1964) 234.
11. Ederer, D.L., Phys.Rev.Letters 13 (1964) 760.
12. Samson, J.A.R., Adv.in Atomic and Molec.Physics, Vol.2, Academic Press (New York, 1966) 177.
13. Haensel, R., Keitel, G., Schreiber, P. and Kunz, C., Phys.Rev. 188 (1969) 1375.
14. Manson, S.T. and Cooper, J.W., Phys.Rev. 165 (1968) 126.
15. Amusia, M.Ya., Cherepkov, N.A. and Chernysheva, L.V., Soviet Physics - JETP 33 (1971) 90.
16. Wendin, G., J.Phys.B (Atom.Molec.Phys.) to be published.
17. Codling, K. and Madden, R.P., Phys.Rev.Letters 12 (1964) 106.
18. Codling, K. and Madden, R.P., Appl.Optics 4 (1965) 1431.
19. Mehlhorn, W., Z.Phys. 187 (1965) 21.
20. Siegbahn, K. and co-workers, ESCA Applied to Free Molecules, North-Holland Publ.Comp. (Amsterdam, 1969).
21. El-Sherbini, Th.M., Van der Wiel, M.J. and De Heer, F.J., Physica 48 (1970) 157.
22. Van der Wiel, M.J., El-Sherbini, Th.M. and Vriens, L., Physica 42 (1969) 411.
23. Van der Wiel, M.J., Physica 49 (1970) 411.

24. Moore, C.E., Atomic Energy Levels, NBS Circular 467, Vol.1, U.S. Government Printing Office (Washington DC, 1949).
25. Stuber, F.A., J.Chem.Phys. 42 (1965) 2639.
26. Carlson, T.A., Phys.Rev. 156 (1967) 142.
27. Cooper, J.W., Phys.Rev.Letters 13 (1964) 762.
28. Wendin, G., Phys.Letters A, to be published.
29. Fink, R.W., Jopson, R.C., Mark, H. and Swift, C.D., Rev.Mod.Phys. 38 (1966) 513.
30. Bhalla, C.P., J.Phys.B (Atom.Mol.Phys.) 3 (1970) 916.
31. Watson, W.S. and Morgan, F.J., J.Phys.B (Atom.Mol.Phys.) 2 (1969) 277.
32. McGuire, E.J., Phys.Rev. 175 (1968) 20.
33. Allen, S.J.M. "X Rays in Theory and Experiment" edited by Compton, A.H. and Allison, S.K. (Van Nostrand, Princeton, New Jersey, 1935).

IONIZATION OF N₂ AND CO BY 10 keV ELECTRONS AS A FUNCTION OF THE ENERGY LOSS

I. VALENCE ELECTRONS

TH. M. EL-SHERBINI and M. J. VAN DER WIEL

FOM-Instituut voor Atoom- en Molecuulfysica, Amsterdam, Nederland

Synopsis

The small-angle inelastic scattering of 10 keV electrons in N_2 and CO has been measured in coincidence with the ions and fragments formed. Continuous oscillator-strength spectra were obtained for the production of N_2^+, $N^+(N_2^{++})$, CO^+, C^+, O^+ and CO^{++}, *via* outer-shell excitations. Besides the onset of excitation to the X, A and B electronic states of N_2^+ and CO^+ (which is observed as an increase in the oscillator strength), the N_2^+ spectrum shows that a considerable fraction of the oscillator strength goes to double electron transitions, *i.e.* to auto-ionizing Rydberg states converging to the C state. The formation of N^+ ions at the lowest threshold for dissociation is discussed with regard to earlier suggestions in literature. In the case of N_2, the mass-14 spectrum (*i.e.* N^+ and N_2^{++}) clearly shows the contribution of N_2^{++} formation at energy losses above 42 eV, while the structure in this range corresponds to onset of ionization to N_2^{++} levels known from Auger-electron spectroscopy. The measurements of CO show that most of the doubly charged ions dissociate to C^+ and O^+ with lifetimes shorter than about 10^{-8}s. Comparison with optical measurements and electron-impact data shows the contribution to the total cosillator strength of fragment ions with excess energy of formation.

1. *Introduction.* Most of the recent progress in the experimental study of excitations in molecules and the subsequent ionization or fragmentation has been made with one of the following methods:

a) The appearance potential technique, often combined with a method for determination of the kinetic energy of fragment ions. This technique[1-4) when applied with sufficiently high energy resolution, is a powerful tool in the study of the potential-energy diagrams of molecules.

b) The photoabsorption technique. In the energy range of the usual continuum-light sources (up to about 20 eV), very high resolution can be obtained, as shown in measurements of the electronic and vibrational states of neutral and singly-ionized molecules[5, 6). The energy range can be extended by the use of line sources[7), at the expense of continuous energy variation, or by the use of electron synchrotron radiation[8). For absolute

64

measurements of photoabsorption cross sections a difficulty is presented by the calibration of the photographic plates or other photon detectors. Furthermore, the final product of the energy absorption is unknown.

c) The technique of photoionization in mass spectrometry, as described for instance in refs. 9–12. The potentialities and the limitations of this method are similar to those of the previous one, but additional information can be obtained from the measurement of the m/e value of the final state.

d) Photoelectron spectroscopy. This technique has been extensively developed for the study of electron-orbital energies of atoms and molecules. It gives information only about the states excited in the initial energy absorption (see for a review refs. 13 and 14).

e) Auger-electron spectroscopy (induced by fast electrons). This technique was used recently[14,15] for the determination of the electronic states of doubly ionized molecules, produced *via* inner-shell ionization. It provides energy differences and therefore it may be difficult in some cases to obtain an unambiguous assignment of the initial and final states.

In the work described in this paper we have used a method which is essentially similar to that of photoionization (c). A photon source of variable energy is simulated by observing the energy loss of fast electrons, scattered through a small angle; the correlation between energy transfer and ion formation is determined by coincidence detection of the scattered electron and the corresponding ion. This method, developed earlier for the study of multiple ionization of the noble gases[16,17,18] produces relative oscillator strengths by apllication of the first Born relation for electron scattering at small momentum transfers.

Our aim has been to make a quantitative study of the oscillator strength for ionization and dissociation of simple molecules over a wide range of continuously variable energy transfers, with moderate energy resolution. This specific aspect of the energy absorption by molecules, which can be for instance a sensitive test for molecular continuum wavefunctions, has been rather neglected in some of the studies [of a more spectroscopic nature, see (c)], due to the difficulties mentioned. N_2 and the iso electronic CO were studied, since a vast amount of information on these molecules is already available.

Finally, it might be emphasized that in the present data the final states are only characterized by their m/e value. Much more information should be obtained if also the radiative decay of the excited states of the ions could be observed. We are now in the process of modifying the apparatus such that triple coincidences between scattered electrons, ions and photons can be detected.

2. *Experimental.* 2.1. A p p a r a t u s   a n d   d e r i v a t i o n   o f   o s c i l l a t o r s t r e n g t h s. The main features of the electron–ion coincidence experiment
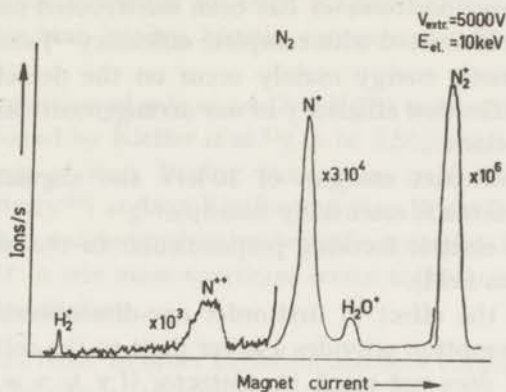
Fig. 1. Mass spectrum of N_2.

have been described in detail in previous publications [16,17,19]. In brief, a 10 keV electron beam is crossed by a beam of neutral gas molecules (pressure about 10^{-5} torr). Ions formed in the collision are extracted by a homogeneous extraction field and charge-analysed. Electrons scattered through a small angle (about 5×10^{-3} rad) are decelerated in a retarding lens and energy-selected. The output pulses of the two-particle detectors are fed into a delayed coincidence circuit. The true coincidences, after being separated from the simultaneously registered accidental coincidences, are stored in a data collector [20], which drives the energy-loss scanning.

The resolution of the mass spectrometer is not sufficient to permit the use of $^{14}N^{15}N$ for a separation of the N^+ and N_2^{++} spectra. When measuring CO, the C^+ and O^+ peaks are not fully separated from that of CO^{++} due to the excess kinetic energy of these fragments. However, there is sufficient separation among the three peaks in the delay spectrum. The amount of mass-14 ions from the N_2 background is smaller than that of CO^{++} by a factor of 1000; also the contribution of O^+ from the background gas H_2O is negligible with respect to that of O^+ from CO.

From the measured intensities of scattering we derive relative oscillator strengths by a method described at length in ref. 16, which essentially consists of multiplying the scattering intensities by K^2, K being the magnitude of the momentum transfer of the projectile electron, while also correcting for the resolution of the angular selection.

2.2. Excess energy of dissociation. In general an excitation to repulsive ionic states will result in the formation of fragment ions with initial kinetic energy. The effect of velocity components normal to the motion through a mass spectrometer is to broaden the peaks (see N_2 mass spectrum, fig. 1) and to reduce the collection efficiency for such fragments, since some of them fail to pass through the slit system of the ion source or that of the

detector. Our mass spectrometer has been constructed such that thermal-energy ions are transmitted with complete efficiency[19]) and such that losses due to initial kinetic energy mainly occur on the detector slit. A rough estimate of the collection efficiency of our arrangement can be made on the following assumptions:

1) At electron-impact energies of 10 keV the angular distribution of dissociative fragments is essentially isotropic[21]).

2) There is no electric focusing perpendicular to the main orbit (homogeneous extraction field).

3) We neglect the effect of first-order one-dimensional focusing of the magnet. This assumption provides a lower limit to the collection efficiency.

4) A fragment does not reach the detector if $v_\perp t_t > w$, where $v_\perp$ is the average velocity normal to the motion through the mass spectrometer, t_t is the time of flight through the mass spectrometer and w is the width (or height) of the detector slit.

We then arrive at an approximate efficiency η given by:

$$\eta \approx 1 - \left[1 - \frac{eV_{extr}}{E_{kin}}\left(\frac{w}{C}\right)^2\right]^{\frac{1}{2}}, \tag{1}$$

where e is the charge of the ion, C is an apparatus constant and η equals 1 for values of $eV_{ex}/E_{kin}(w/C)^2$ larger than 1. For two values of V_{extr} this efficiency has been plotted as a function of E_{kin} in fig. 2.

The distribution of kinetic energies of fragments due to dissociative ionization has been the subject of a series of investigations[21, 22, 23]). Summarizing the results of these studies, which are of interest for the present work, we can say that at electron-impact energies of 100 eV or higher:
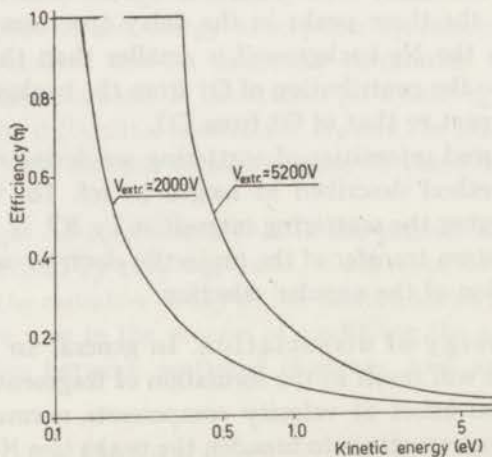

Fig. 2. Collection efficiency for energetic ions as a function of their excess energy of formation.

a) 20% of the total ionization for both N_2 and CO is due to dissociative ionization, the ions having kinetic energies > 0.25 eV, according to Rapp et al.[22]);

b) in N_2 the production of $m/e = 14$ (N^+, N_2^{++}) ions with kinetic energies < 1 eV was found by Kieffer et al.[21]) to be 3.5% of the total ionization; a second group of ions, having more than 1 eV kinetic energy, was reported by Berry[23]) and by Kieffer and Van Brunt[21]).

When taking into account our estimated efficiency (fig. 2), the (N^+, N_2^{++})/ N_2^+ ratio of 0.027 in our mass spectrum seems to be compatible with the results from earlier studies.

2.3. Normalization. In order to obtain absolute values for the oscillator strengths, which enable us to compare our results with optical data, our relative measurements for the parent ions N_2^+ and CO^+ have been normalized on an absolute value of df/dE obtained from photoionization measurements at one particular energy (see ref. 16). Some conditions have to be considered in choosing this energy: a) this energy should lie above the first ionization potential and below the potential for dissociative ionization or multiple ionization; b) no sharp structure is present near this energy within the energy pass width of the analyser; c) the coincidence signal is high enough to permit an accurate measurement.

For N_2^+ and CO^+ we normalized our relative df/dE on the absolute photo-ionization cross sections of Samson and Cairns[24, 25]) at 21.5 eV and 23.6 eV, respectively. For the normalization of the spectra of the dissociative fragments and multiply ionized molecular ions we must consider the following. Our normal procedure[17]) of taking data consists of recording the number of true coincidences per number of ions arriving at the detector, for the reason of eliminating the effect of variations in the electron-beam intensity or the target-gas density. This is actually an internal normalization on the number of interactions taking place. Thus we are able to put the relative df/dE spectra for all ions on the same absolute scale as that of the parent ion N_2^+ (or CO^+), by introducing the relative abundances of the ions as measured from the mass spectrum. This procedure is applicable even in the case of ions formed with initial kinetic energy, with the restriction that the result gives the absolute value of the oscillator strength, weighted at each energy transfer with an efficiency factor (fig. 2), depending on the kinetic energies of the ions produced at that particular energy transfer. By recording the spectra at different extraction voltages, the contribution of energetic fragments can be assessed (see section 3.2.2).

3. *Results and Discussion.* 3.1. General. Oscillator strengths for the formation of N_2^+, N^+ (N_2^{++}), CO^+, C^+, O^+ and CO^{++} *via* excitation of the valence electrons of N_2 and CO have been measured in the region of energy

transfers between treshold and 60 eV. For ions formed at thermal energies absolute values are given, normalized on Samson and Cairns's photoionization data (refs. 24 and 25), while for fragment ions with excess energy of formation, the values represent the true oscillator strength reduced by the collection efficiency of the mass spectrometer [eq. (1)]. The data have been plotted in figs. 3–8, and for N_2^+ and CO^+ numerical results are given in table I. The intensity of electrons scattered in coincidence with N^{++}, C^{++} and O^{++} appeared to be too low to obtain reasonable spectra. Potential-energy diagrams of the two molecules are shown in fig. 9.

TABLE I

Oscillator strengths for N_2^+ and CO^+

Energy loss E (eV)	N_2^+ (in 10^{-2} eV^{-1})	E (eV)	N_2^+ (in 10^{-2} eV^{-1})	Energy loss E (eV)	CO^+ (in 10^{-2} eV^{-1})	E (eV)	CO^+ (in 10^{-2} eV^{-1})
14	0.29	38	10.0	12	0.05	40	9.2
16	13.6	40	8.6	14	13.8	42	8.3
18	20.0	42	8.1	16	14.3	44	7.7
20	20.4	44	7.3	18	21.5	46	7.0
22	20.7	46	6.7	20	21.4	48	6.3
24	21.9	48	6.5	22	20.2	50	5.7
26	20.3	50	5.7	24	19.7	52	5.6
28	19.6	52	5.9	26	18.6	54	5.2
30	18.3	54	5.7	28	17.3	56	4.3
32	15.6	56	4.6	30	15.4	58	3.9
34	13.6	58	4.1	32	13.7	60	3.6
36	11.6	60	3.6	34	12.6		
				36	11.5		
				38	10.7		

$\int_{15.6 \text{ eV}}^{60} \frac{R}{E} \frac{df}{dE} dE$ (this work)[†]	$\int_{15.6 \text{ eV}}^{\infty} \frac{R}{E} \frac{df}{dE} dE$ (Schram)[††]	$\int_{14.0 \text{ eV}}^{60} \frac{R}{E} \frac{df}{dE} dE$ (this work)[†]
2.91	3.08	2.89

[†] The contribution from 60 eV till ∞ is estimated by extrapolation of our curve to be less than 5%.
[††] See section 3.4.

3.2. Nitrogen. 3.2.1. N_2^+. The spectrum of N_2^+ formation, shown in fig. 3, was recorded with a resolution of 0.5 eV FWHM. The onset of ionization to the $X^2\Sigma_g^+$, $A^2\Pi_u$ and $B^2\Sigma_u^+$ states of this ion, corresponding to ejection of a $\sigma_g 2p$, $\Pi_u 2p$ and $\sigma_u 2s$ electron[†], respectively, appears as jumps

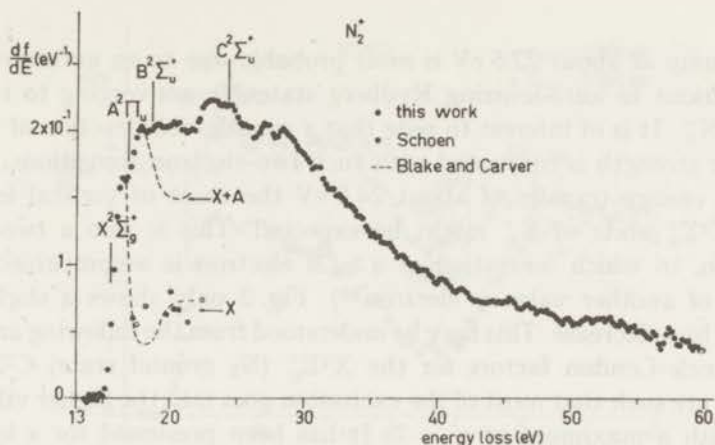[†] See Herzberg [26] for nomenclature of electron orbitals.

Fig. 3. Oscillator-strength spectrum of N_2^+.

in our curve at energies in agreement with the vertical appearance potentials measured spectroscopically or with electron impact. It is interesting to compare the relative intensities of excitation to each of the three states at threshold with the intensities at higher energy transfers as determined by means of photoelectron spectroscopy. In a limited range of energies above threshold these intensities have been determined by Schoen[27] and with higher accuracy by Blake and Carver[28]. Our relative intensities at threshold are in agreement with the results of the latter authors, which have further been used to indicate the contribution of each of the three N_2^+ states to our df/dE spectrum (fig. 3, dashed lines). Besides, Siegbahn *et al.*[14], using $M_gK_\alpha X$ rays (1254 eV), found the absorption to the X, A and B states to produce photoelectron lines with relative intensities 0.16, 0.12 and 0.72, respectively. Since this B state fraction is quite different from that near threshold, and since further at very high energy transfers df/dE is expected to behave as $E^{-\frac{5}{2}}$[29]), we must conclude that the contribution of absorption to the B state becomes largely dominant at intermediate energies. The only other data pertaining to this subject are those representing the integral of $(R/E)(df/dE)$ over the whole continuum, *i.e.*,

$$\int_{I.P.}^{\infty} \frac{R}{E} \frac{df}{dE} \, dE \qquad (R \text{ is Rydberg energy}),$$

as determined from total emission cross sections for fast electron impact by Aarts and de Heer[30,31]: about 0.7 for the X state, about 2.0 for the A state and 0.51 for the B state. These values also show that the relative intensity of excitation to the B state cannot be dominant in the range of energy transfers near threshold, which contributes ($\approx 1/E$) to the integral with a large weight.

The bump at about 22.5 eV is most probably due to an unresolved series of transitions to auto-ionizing Rydberg states[32]), converging to the $C^2\Sigma_u^+$ state of N_2^+. It is of interest to note that a considerable fraction of the total oscillator strength is connected with such two-electron transitions.

At an energy transfer of about 24.5 eV the onset of vertical ionization to the $C^2\Sigma_u^+$ state of N_2^+ might be expected. This is also a two-electron transition, in which ionization of a $\sigma_u 2s$ electron is accompanied by excitation of another valency electron[33]). Fig. 3 only shows a slight bump followed by a decrease. This may be understood from the following argument: The Franck–Condon factors for the $X^1\Sigma_g^+$ (N_2 ground state)–$C^2\Sigma_u^+$ transition[34]) are such that most of the excitation goes into the higher vibrational levels with a maximum at $v' = 7$. It has been presumed for a long time already[35, 36]) that for vibrational levels with $v' \geq 3$ or 4 predissociation might occur. A recent experiment on collision-induced dissociation of N_2^+ by Fournier et al.[37]) confirms the suggestion of Albritton et al.[38]), that a rapid predissociation of the $C^2\Sigma_u^+$ state occurs for values of $v' \geq 4$, which is 20 times more probable than radiative decay. Therefore no onset is to be expected in the N_2^+ spectrum, but rather in that of N^+ (see section 3.2.2).

The structure around 28 eV was observed earlier by Dromey et al.[39]) in the first differential ionization efficiency of N_2^+ and by Samson and Cairns[24]) in photoabsorption. Since no one-electron ionization onset is possible in this range, the structure must be due to excitation to auto-ionizing states or simultaneous excitation and ionization to states like the $C^2\Sigma_u^+$ state. In the same energy region similar structure is observed in the CO^+ spectrum (see section 3.3.1).

The highest one-electron ionization threshold of the valency shell, that of the $\sigma_g 2s$ electron, is expected to lie at 37.3 eV according to the binding-energy determination of this electron by Siegbahn et al.[14]). They suggested that the large width of the $\sigma_g 2s$ photoelectron peak (about 3 eV) might be due to vibrational structure and also to Coster–Kronig processes. On the other hand Aarts and de Heer[40]), from a study of the radiative decay of excited N^+ ions, proposed that the one-electron ejection from the $\sigma_g 2s$ orbital leads to dissociation of the N_2 molecule. If this is so, no onset due to $\sigma_g 2s$ ionization is to be expected in the N_2^+ curve, and none is observed (see also section 3.2.2 for N^+ production). Coster–Kronig processes are ruled out, since they should leave the ion in one of the doubly ionized states, the lowest of which is known to pass the ground-state Franck–Condon region at an energy of 42.7 eV.

3.2.2. $N^+(N_2^{++})$. Fig. 4 represents the oscillator-strength spectrum of $N^+(N_2^{++})$ ions between the lowest threshold and 60 eV (energy resolution 2.0 eV FWHM). Two sets of measurements at two different extraction voltages were plotted in the figure to show the contribution of ions with
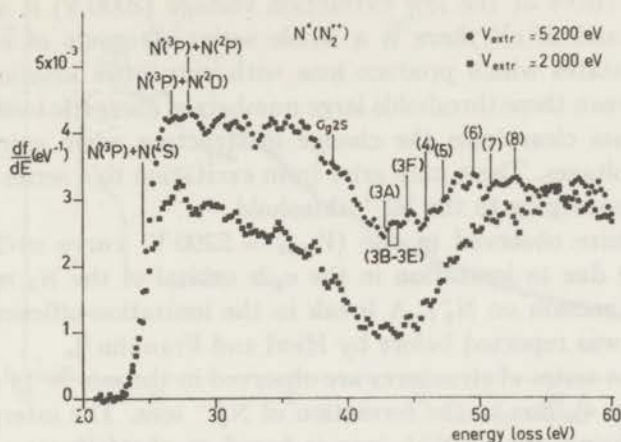
Fig. 4. Oscillator-strength spectrum of $N^+(N_2^{++})$, recorded at two different ion extraction voltages. The numbers between brackets refer to the lines in the Auger spectrum of Siegbahn et al.[14]).

initial kinetic energy (this was discussed in section 2.2). Frost and McDowell[3]), using the R.P.D. method obtained values of 24.32, 26.66 and 27.93 eV for the appearance potentials of N^+ ions in the ground state (^{3}p state) from three distinct processes. At the thresholds of these processes an increase in the oscillator strength is observed in our curve.

There has been some discussion in the literature [41, 36, 4]) about the formation of N^+ at 24.3 eV (the lowest threshold of this ion). The two most likely processes are predissociation of the $C^2\Sigma_u^+$ state of N_2^+ or excitation to the vibrational continuum of the $D^2\Pi_g$ state. The former process was suggested by McDowell[41]) and by Carroll[36]), while the latter was proposed by Hierl and Franklin[4]) and by Aarts and de Heer[40]) who expect that vertical transitions from the ground state will reach parts of the $D^2\Pi_g$ potential-energy curve above the dissociation limit at 24.3 eV. From our experiment we can only put an upper limit to the lifetime of a possible intermediate N_2^+ state. If the lifetime of such a state is larger than about 20 ns, the N^+ ions formed will reach the ion detector with a measurably different time of flight than normal N^+ ions. Our measurements of the time of flight of N^+ fragments at threshold (24.3 eV) appeared to agree with the value expected for an $m/e = 14$ ion within the accuracy of the measurements ($\pm$ 5 ns). This puts an upper limit to the lifetime of a possible intermediate N_2^+ state of 20 ns. We already quoted an earlier experiment[37]) giving a lifetime for the C state of about 5 ns. The possibility that N^+ production at the lowest threshold arises from excitation to the $C^2\Sigma_u^+$ state, is also left open when we consider the height of the threshold jump. This jump appears to be of the same order of magnitude as that of the corresponding two-electron transitions at 22.5 eV in the N_2^+ spectrum.

From the curve at the low extraction voltage (2000 V) it appears that between 28 and 37 eV there is a whole series of onsets of excitation to dissociative states which produce ions with very little kinetic energy. At energies between these thresholds large numbers of energetic ions are formed, which becomes clear from the change in structure when going to higher extraction voltages. These may arise from excitation to a series of repulsive N_2^+ states, converging to the N_2^{++} threshold.

The structure observed in the ($V_{extr} = 5200$ V) curve of $N^+(N_2^{++})$ at 39 eV can be due to ionization in the $\sigma_g 2s$ orbital of the N_2 molecule (see the previous section on N_2^+). A break in the ionization-efficiency curve of N^+ at 39 eV was reported before by Hierl and Franklin[4]).

A rise and a series of structures are observed in the $m/e = 14$ curve above 42 eV (see fig. 4), due to the formation of N_2^{++} ions. The interpretation of this rise as being due to N_2^{++} ions is based on the following arguments:

a) The shape of the rise resembles the general shape for the continuum of doubly ionized ions, *i.e.* an extended rise from $df/dE = 0$ to a broad maximum (see for Ar, He and Ne refs. 17 and 18), while the series of structures observed in the curve can be identified as onsets of ionization to N_2^{++} levels known from calculations[42]) and Auger-electron spectroscopy[14, 15]) (see the lines indicating these levels in fig. 4). So it appears that in excitation from the ground state the same N_2^{++} levels are populated as in the Auger decay from a K-shell ionized state (N_2^{K+}). From this it follows that the potential-energy curve of the N_2^{K+} state is quite similar to that of the ground state, *i.e.* the K electrons hardly contribute to the molecular bonding. Two values for the appearance potential of N_2^{++} ions were obtained previously in mass spectrometry, namely 42.7 and 43.8 eV[43]).

b) The two curves of fig. 4 show that the oscillator strength is almost independent of the extraction voltage at energy losses around 60 eV. This indicates that most of the ions formed in this energy-loss range have only thermal energies (*i.e.* N_2^{++} ions).

c) In our CO measurements, we obtained a CO^{++} spectrum of a similar shape (see section 3.3.4).

This N_2^{++} contribution must show up as a bump in the photoabsorption spectrum. This was observed by de Reilhac and Damany[7]), who measured the absorption coefficients of N_2 in the far ultraviolet (31–124 eV).

A clear jump is obtained in the $V_{extr} = 5200$ V curve at 47.5 eV, the threshold energy for excitation to the $A^3\Pi_g$ state of N_2^{++} (see fig. 4, peak 5). The dissociation of this state into two N^+ ions with considerable kinetic energy was predicted by Hurley[42]) and verified experimentally by Hierl and Franklin[4]) who observed a sudden increase in the translational energy of the N^+ ions at an electron energy of 48 ± 2 eV.

3.3. Carbon monoxide. 3.3.1. CO$^+$. The oscillator-strength spectrum of CO$^+$ is shown in fig. 5 (energy resolution 0.5 eV FWHM) and can be seen
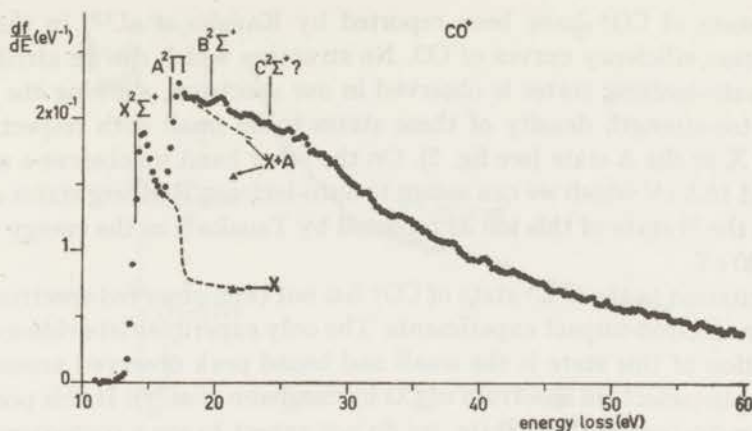
Fig. 5. Oscillator-strength spectrum of CO⁺.
● this work; --- Schoen; ▲ Al-Joboury et al.

to resemble quite closely that of N_2^+. At the onset energies of ionization to the three well known electronic states of this ion, namely the $X^2\Sigma^+$, $A^2\Pi$ and $B^2\Sigma^+$ states, an increase in the continuous oscillator strength is observed. These onset energies were obtained before in electron impact and photo-absorption measurements [4,5,44]. With respect to the relative intensities of excitation to each of these states, there are a few values available in the literature. In a photoelectron experiment Schoen [27] has measured the percentage of excitation to these states as a function of the incident photon energy in the energy range between 12–23 eV. Within the (limited) accuracy of his experimental results (30% for the A state and 100% for the B state), his percentages of excitation to the three states are in agreement with the values obtained from similar measurements by Al-Joboury et al. [44] at 21.21 eV. In fig. 5 we used Schoen's results to indicate the contribution of each of the three CO⁺ states to the oscillator-strength spectrum (fig. 5, dashed lines), while the figure also contains the values of Al-Joboury et al. [44] at 21.21 eV. From the photoelectron spectrum by Siegbahn et al. [14] of CO excited by MgK_α radiation (1254 eV) values of 0.26, 0.14, 0.60 are obtained for the relative intensities of the absorption to the X, A and B states respectively. From the difference between their result for the B-state fraction and those of Schoen and Al-Joboury et al. near the threshold of CO⁺, we can conclude (see for N_2^+ section 3.2.1), that the contribution of absorption to the B state becomes largely dominant at intermediate energies. Furthermore, the results of Aarts and de Heer [30,31] for $\int_{I.P.}^\infty (R/E)(df/dE)\,dE$ being about 0.9 for the X state, 2.7 for the A state and 0.82 for the B state show that the B state cannot be dominant in the range of energy transfers near threshold, since excitation in this range contributes with a large weight ($\sim 1/E$) to the integral.

Auto-ionizing peaks assigned to various Rydberg series converging to the

A$^2\Pi$ state of CO$^+$ have been reported by Kaneko *et al.*[12]) in the photo-ionization efficiency curves of CO. No structure which can be attributed to such auto-ionizing states is observed in our spectrum, showing the average oscillator-strength density of these states to be small with respect to that of the X or the A state (see fig. 5). On the other hand we observe a structure around 18.5 eV which we can assign to auto-ionizing Rydberg states converging to the B state of this ion as reported by Tanaka[5]) in the energy range of 17.7–20 eV.

Excitation to the C$^2\Sigma^+$ state of CO$^+$ has not been observed spectroscopically or in electron-impact experiments. The only experimental evidence for the formation of this state is the small and broad peak observed around 24 eV in the photoelectron spectrum of CO by Siegbahn *et al.*[14]). If this peak is due to an excitation to the C state, we do not expect to see a corresponding rise in our spectrum, since the equilibrium separation of this state was calculated[45]) to be 0.2 Å greater than that for CO in the ground state and therefore a vertical transition from the ground state will populate the vibrational continuum of this state and dissociation occurs.

The structures around 26 eV are similar to those in the N$_2^+$ spectrum around 28 eV (see section 3.2.1) and can be due to excitation to auto-ionizing states or due to simultaneous excitation and ionization.

The highest one-electron ionization threshold of the valency shell, that of the 1σ electron, was found to lie at 38.3 eV according to the binding-energy determination of this electron by Siegbahn *et al.*[14]). The width of this line ($\approx$ 3 eV) which is large with respect to that of the other valency-electron lines of the CO molecule, is probably due to excitation to a repulsive state, since no clear jump is observed at the 1σ-electron energy in our curve (see also section 3.2.1 for N$_2^+$). This conclusion is confirmed by the structures around 39 eV in the spectrum of C$^+$.

3.3.2. C$^+$. The oscillator-strength spectrum of the C$^+$ ion between its lowest threshold and 60 eV (energy resolution 2.0 eV FWHM, $V_{extr} = 5200$ V) is shown in fig. 6. The three appearance potentials for this ion known from the literature[4, 46]) (20.9, 22.45, 24.5 eV) are indicated in the spectrum. The onset at the first appearance potential (20.9 eV) is rather small compared with those at the second and third potentials (see fig. 6). This is understandable since at the first threshold the ion–pair process (C$^+$ + O$^-$) occurs[47]), *i.e.* a discrete excitation to an unstable neutral state (lying in the ionization continuum of CO) as opposed to the continuum excitation of ionized states at the second and third thresholds. The smallness cannot be due to kinetic energy since C$^+$ was observed[4, 23]) to be formed with near-zero kinetic energy at all three appearance potentials. The smooth and extended rise in the spectrum above the second and third appearance potentials cannot be due to excitation to a large energy range of the vibrational continua of the
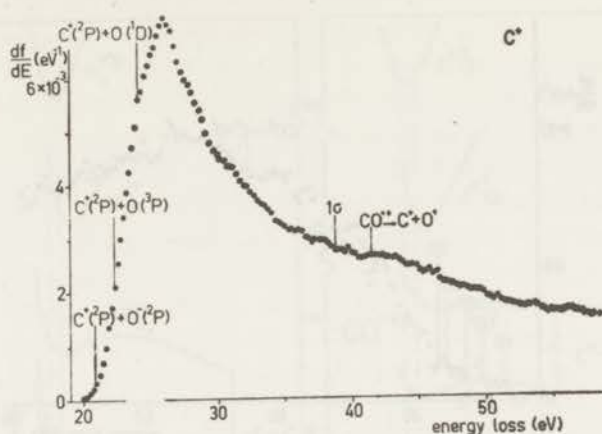
Fig. 6. Oscillator-strength spectrum of C⁺.

X, A and B electronic states of CO^+, since the Franck–Condon factors of transitions to the vibrational continua of these states[46] are essentially equal to zero. The only alternative possibility is that of excitation to repulsive-energy curves, crossing the Franck–Condon region at energies near the dissociation limit.

The structure around 39 eV can be ascribed to the dissociation of the CO^+ state which arises from a hole in the 1σ orbital.

Above 42 eV (CO^{++}: I.P. = 41.8 eV) the spectrum shows the shape of a new continuum that may be due to excitation to short-lived ($< \approx 10^{-8}$ s) dissociative CO^{++} states (see section 3.3.4). This is confirmed by the appearance of a continuum at the same energy region in the O^+ spectrum (see fig. 7) (O^+ is the second product of the dissociation) with a height of the same order of magnitude as that of the C^+ continuum.

3.3.3. O^+. Fig. 7 shows the oscillator-strength spectrum of the O^+ ion between its lowest threshold and 60 eV (energy resolution of 2.0 eV FWHM, V_{extr} = 5200 V). A number of appearance potentials for the formation of this ion is indicated in the curve. These potentials were obtained from spectroscopic calculations and were confirmed experimentally by Hierl and Franklin[4]. In general the O^+ spectrum shows a very slow rise to the maximum with a lot of structure, which indicates that many successive states are involved in the formation of this ion.

Above 42 eV a new continuum starts to appear, which coincides with the one observed before in the C^+ spectrum and is attributed to CO^{++} dissociative states. The rise to this continuum ($\approx 3 \times 10^{-4}$ eV^{-1}) is somewhat larger than that of the C^+ continuum ($\approx 2 \times 10^{-4}$ eV^{-1}) as should be expected on the basis of momentum conservation. The velocity of the O^+ ion is $\frac{3}{4}$ of that of the C^+, for which reason O^+ is collected with higher efficiency.
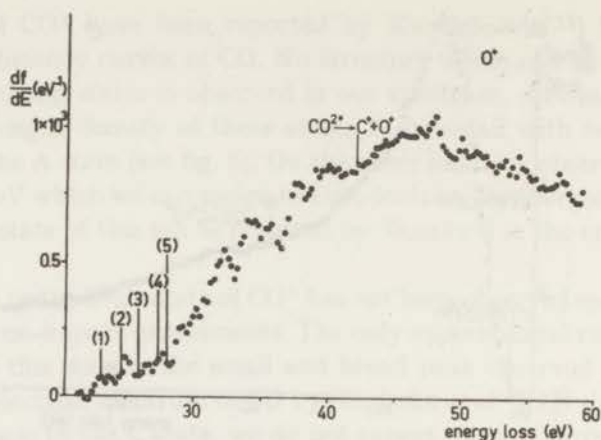
Fig. 7. Oscillator-strength spectrum of O^+. The numbers between brackets refer to the following thresholds; (1): $O^+(^4S) + C^-(^4S)$; (2): $O^+(^4S) + C(^3P)$; (3): $O^+(^4S) + C(^1D)$; (4): $O^+(^4S) + C(^1S)$; (5): $O^+(^2D) + C(^2P)$.

3.3.4. CO^{++}.

The oscillator-strength spectrum of the CO^{++} ion is shown in fig. 8 between its lowest threshold and 75 eV (energy resolution 2.0 eV FWHM, $V_{extr} = 5200$ V). The curve shows the general shape of a double ionization curve, *i.e.* an extended rise from $df/dE = 0$ at threshold to a broad maximum (see for Ar, He and Ne refs. 17 and 18). The difference with the N_2^{++} contribution to the $m/e = 14$ spectrum of N_2 is the much smaller oscillator strength (3×10^{-4} against 3×10^{-3} eV^{-1} in N_2). This is an indication that a large fraction of the various states of this ion dissociates to give C^+ and O^+ ions.

At the energies of the most pronounced structures we have indicated some CO^{++} levels or groups of vibrational levels (see the lines indicating these
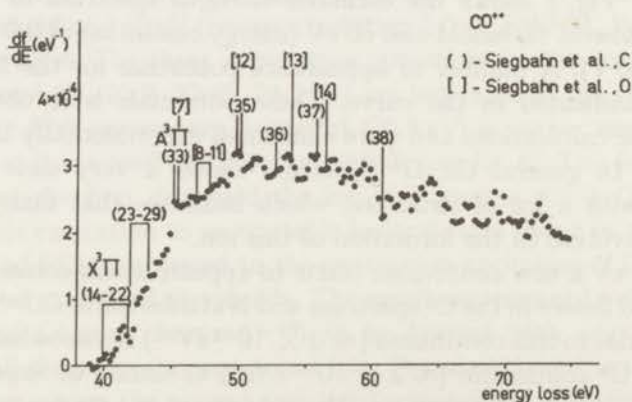

Fig. 8. Oscillator-strength spectrum of CO^{++}. The numbers between brackets refer to the carbon and oxygen Auger lines in the spectra of Siegbahn *et al.*[14]).
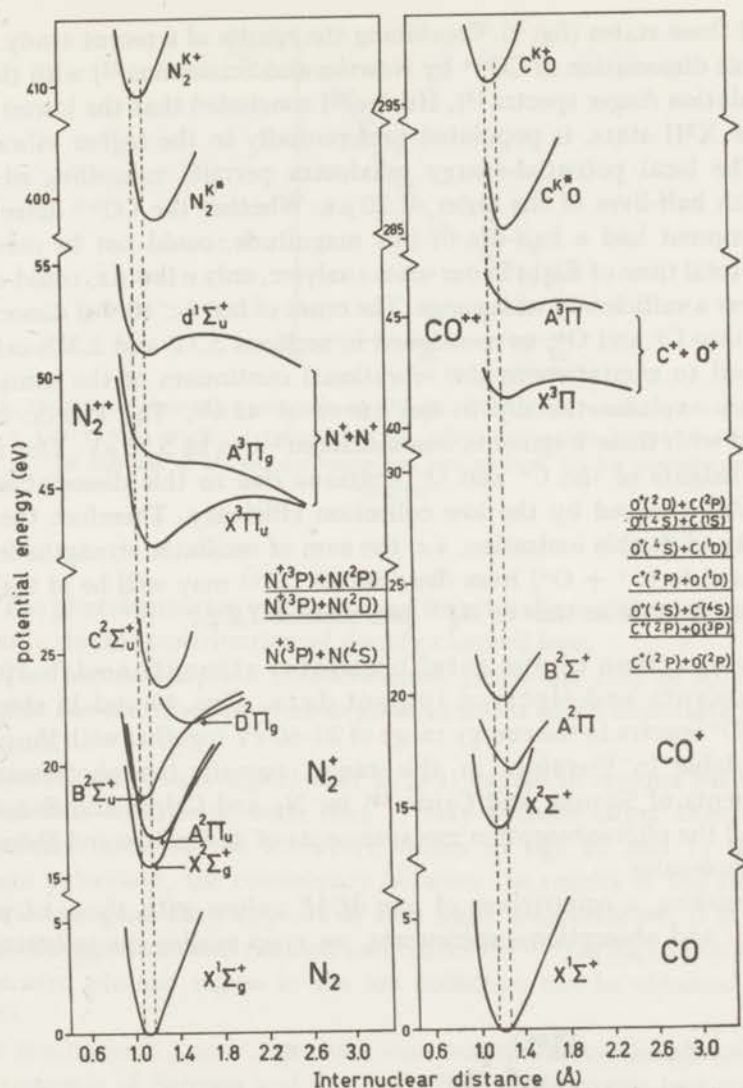
Fig. 9. Potential energy diagrams of N_2 and CO. Data were taken from refs. 26, 50, 15 and 46; for N_2^{++} only a few of the known levels [15] have been plotted. The K-shell processes are discussed in the next paper (II).

levels in fig. 8) as obtained from measurements by Siegbahn et al.[14] of the carbon and oxygen Auger spectra of CO. A partial assignment of these levels was made recently by Moddeman et al.[48], from similar measurements. Two of these levels were observed before in mass spectra[49] with the appearance energies of 41.8 eV and 45.9 eV. It was suggested by Hurley[50] that these two states are the $X^3\Pi$ state (the ground electronic state of this ion) and the $A^3\Pi$ state, on the basis of a calculation of the potential-energy

curves of these states (fig. 9). Combining the results of a recent study of the metastable dissociation of CO^{++} by Newton and Sciamanna[51]) with those of high resolution Auger spectra[14]), Hurley[50]) concluded that the lowest CO^{++} state, the X^{3}Π state, is populated preferentially in the higher vibrational levels. The local potential-energy maximum permits tunnelling of these levels with half-lives of the order of 20 μs. Whether the CO^{++} detected in our experiment had a half-life of this magnitude, could not be measured since the total time of flight in our mass analyser, only a few μs, could not be varied over a sufficiently wide range. The onset of fast ($<$ 10^{-8} s) dissociation of CO^{++} into C$^+$ and O$^+$, as mentioned in sections 3.3.2 and 3.3.3, can now be ascribed to excitation to the vibrational continuum of the same X^{3}Π state. This explains the dip in our curve at 42 eV. The kinetic energy associated with these fragments was measured[51]) to be 5.75 eV. This means that the heights of the C$^+$ and O$^+$ continua due to this dissociation, are considerably reduced by the low collection efficiency. Therefore the total probability of double ionization, *i.e.* the sum of oscillator strengths leading to CO^{++} and to (C$^+$ + O$^+$) from dissociative CO^{++} may well be of the same order of magnitude as that of N$_2^{++}$ (see section 3.2.2.).

3.4. **Comparison of our total oscillator strengths with optical measurements and electron impact data.** Figs. 10 and 11 show our N$_2^+$ and CO$^+$ spectra in the energy range of 20–60 eV together with the optical data available in literature in this range, namely the photoionization measurements of Samson and Cairns[24]) for N$_2$ and Cairns and Samson[25]) for CO and the photoabsorption measurements of de Reilhac and Damany[7]) for both molecules.

When making a comparison of our df/dE values with those of photoionization- and absorption experiments, we must realize the following:
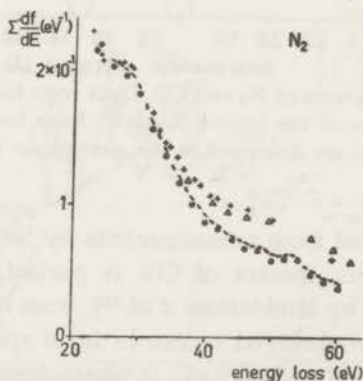

Fig. 10. Oscillator-strength spectrum of N$_2$. ● : N$_2^+$, this work; ----: N$_2^+$ + N$^+$(N$_2^{++}$), this work; + : Samson *et al.*, photoionization (total charge measurement); △ : de Reilhac *et al.*, photoabsorption (see section 3.4 for discussion of various results).
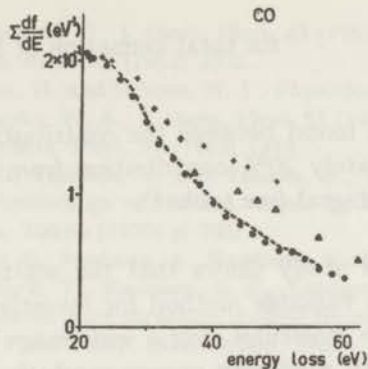
Fig. 11. Oscillator-strength spectrum of CO. [●] : CO⁺, this work; -----: CO⁺ + C⁺ + O⁺ + CO⁺⁺, this work; + : Cairns *et al.*, photoionization (total charge measurement); △ : de Reilhac *et al.*, photoabsorption (see section 3.4 for discussion of various results).

1) The photoionization values derived from total ion current measurements contain a double contribution of doubly charged ions.

2) The photoabsorption measurements yields the sum of df/dE for all ions, plus the contribution of absorption to states which dissociate to neutral fragments.

Therefore we should expect that 2) ≥ 1) except in regions where doubly charged ions contribute, such that 1) may become larger than 2). Since the general trend of the literature values in figs. 10 and 11 shows the opposite behaviour, the consistency between the results of the two experiments is less good than appears at first sight. Furthermore, it is not clear how in the experiments of Samson and Cairns [24, 52, 25] at high photon energies a saturated plateau region in the ion collection can be obtained (see also ref. 16).

Our results for N_2^+ and CO⁺ which were normalized on the photoionization measurements of Samson and Cairns [24, 25] at low energies (see section 2.3) are considerably lower than the earlier data at high energies. These deviations must be attributed to fragment ions which are formed with excess kinetic energies. The existence of such a large contribution of energetic fragments is known already from the work of Rapp *et al.*[22], who found that a large fraction (20%) of the total ionization of N_2 and CO by electron impact (electron energy ≥ 100 eV) is due to dissociative ionization. If we add the contribution of the other ions (N^+, N_2^{++} and C⁺, O⁺, CO⁺⁺) to the two curves, we obtain the dashed curves (figs. 10 and 11), which clearly demonstrate the effect of the small collection efficiency of the energetic ions in our apparatus.

In an electron impact experiment Schram [53] has obtained the integral:

80

$$\int_{\text{I.P.}}^{\infty} \frac{R}{E} \frac{df}{dE} dE \qquad \text{for total ionization of } N_2.$$

A good agreement is found between the contribution of N_2^+ to the integral (assuming approximately 20% contribution from the other ions) and our results for the N_2^+ integral (see table I).

4. *Conclusion.* Our study shows that the scattered electron–ion coincidence technique is a valuable method for investigating the ionization and dissociation of simple molecules over a wide range of continuously variable energy transfers, with moderate energy resolution. Double electron transitions have been reported to contribute with a considerable fraction to the N_2^+ oscillator-strength spectrum. With respect to the formation of N^+ at the lowest threshold (24.3 eV) *via* an intermediate N_2^+ state, our measurements give an upper limit to the lifetime of such a state of 20 ns. The contribution of N_2^{++} to the $m/e = 14$ spectrum of N_2 is observed above 42 eV. The measurements of CO show that most of the doubly charged ions (CO++) dissociate to C^+ and O^+ with lifetimes shorter than about 10^{-8}s. Triple-coincidence measurements are proposed for more detailed studies of the excited states in molecules.

REFERENCES

1) Fox, R. E., Hickam, W. M., Kjeldaas, T. and Grove, D. J., Phys. Rev. **84** (1951) 859.
2) Hagstrum, H. D., Rev. mod. Phys. **23** (1951) 185.
3) Frost, D. C. and McDowell, C. A., Proc. Roy. Soc. (London) **236** (1956) 278.
4) Hierl, P. M. and Franklin, J. L., J. chem. Phys. **47** (1967) 3154.
5) Tanaka, Y. and Takamine, T., Sci. Pap. I.P.C.R. **39** (1942) 427; Tanaka, Y., Sci. Pap. I.P.C.R. **39** (1942) 447.
6) Huffman, R. E., Larrabee, J. C. and Tanaka, Y., J. chem. Phys. **40** (1963) 2261.
7) De Reilhac, L. and Damany, N., J. Phys. (1971), to be published.

8) Codling, K. and Madden, R. P., J. chem. Phys. **42** (1965) 3935.

9) Schoen, R. I., J. chem. Phys. **37** (1962) 2032.

10) Cairns, R. B., Harrison, H. and Schoen, R. I., Phys. Rev. **183** (1969) 52.

11) Berkowitz, J. and Chupka, W. A., J. chem. Phys. **51** (1969) 2431; Chupka, W. A. and Berkowitz, J., J. chem. Phys. **51** (1969) 4244.

12) Kaneko, T., Omura, I., Yamada, Y, and Tanaka, K., Recent Developments in Mass Spectroscopy, Proceedings of the Int. Conf. on Mass Spectroscopy, University of Tokyo Press, Tokyo (1970) p. 751.

13) Siegbahn, K., Nordling, C., Fahlman, A., Nordberg, R., Hamrin, K., Hedman, J., Johansson, G., Bergmark, T., Karlsson, S. E., Lindgren, I. and Lindberg, B., Atomic molecular and solid state structure studied by means of electron spectroscopy, North-Holland Publ. Comp. (Amsterdam, 1967).

14) Siegbahn, K., Nordling, C., Johansson, G., Hedman, J., Hedén, P. F., Hamrin, K., Gelius, U., Bergmark, T., Werme, L. O., Manne, R. and Baer, Y., ESCA applied to free molecules, North-Holland Publ. Comp. (Amsterdam, 1969).

15) Stalherm, D., Cleff, B., Hillig, H. and Mehlhorn, W., Z. Naturforsch. **24a** (1969) 1728.

16) Van der Wiel, M. J., Physica **49** (1970) 411.

17) Van der Wiel, M. J. and Wiebes, G., Physica **53** (1971) 225.

18) Van der Wiel, M. J. and Wiebes, G., Physica **54** (1971) 411.

19) Van der Wiel, M. J., El-Sherbini, Th. M. and Vriens, L., Physica **42** (1969) 411.

20) Ikelaar, P., Van der Wiel, M. J. and Tebra, W., J. Phys. E. **4** (1971) 102.

21) Kieffer, L. J. and Van Brunt, R. J., J. chem. Phys. **46** (1967) 2728.

22) Rapp, D., Englander-Golden, P. and Briglia, D. D., J. chem. Phys. **42** (1965) 4081.

23) Berry, C. E., Phys. Rev. **78** (1950) 597.

24) Samson, J. A. R. and Cairns, R. B., J. Opt. Soc. Amer. **55** (1965) 1035.

25) Cairns, R. B. and Samson, J. A. R., J. Opt. Soc. Amer. **56** (1966) 526.

26) Herzberg, G., Spectra of Diatomic Molecules, 2nd ed., Van Nostrand, (New York, 1966).

27) Schoen, R. I., J. chem. Phys. **40** (1964) 1830.

28) Blake, A. J. and Carver, J. H., J. chem. Phys. **47** (1967) 1038.

29) Kabir, P. K. and Salpeter, E. E., Phys. Rev. **108** (1957) 1256; Rau, A. R. P. and Fano, U., Phys. Rev. **162** (1967) 68.

30) Aarts, J. F. M. and De Heer, F. J., Physica **49** (1970) 425.

31) Aarts, J. F. M. and De Heer, F. J., private communication.

32) Codling, K., Astrophys. J. **143** (1966) 552.

33) Frost, D. C. and McDowell, C. A., Proc. Roy. Soc. **A232** (1955) 227.

34) Nicholls, R. W., J. quant. Spectrosc. radiative Transfer **2** (1962) 433.

35) Douglas, A. E., Canad. J. Phys. **30** (1952) 302.

36) Carroll, P. K., Canad. J. Phys. **37** (1959) 880.

37) Fournier, P., Van de Runstraat, C. A., Govers, T. R., Schopman, J., De Heer, F. J. and Los, J., Chem. Phys. Letters **9** (1971) 426.

38) Albritton, D. L., Schmeltekopf, A. L. and Ferguson, E. E., VI ICPEAC, Book of Abstracts, MIT Press (Cambridge, Mass., 1969) p. 331.

39) Dromey, R. G., Morrison, J. D. and Traeger, J. C., Internat. J. Mass Spectrum. Ion. Phys. **6** (1971) 57.

40) Aarts, J. F. M. and De Heer, F. J., Physica **52** (1971) 45.

41) McDowell, C. A., Applied Mass Spectrometry, The Institute for Petroleum (London, 1954) p. 129.

42) Hurley, A. C., J. molecular Spectrosc. **9** (1962) 18.

43) Dorman, F. H. and Morrison, J. D., J. chem. Phys. **39** (1963) 1906.

44) Al-Joboury, M. I., May, D. P. and Turner, D. W., J. chem. Soc. (1965) 616.
45) Sahni, R. C., Trans. Faraday Soc. **63** (1967) 801.
46) Krupenie, P. H., The Band Spectrum of Carbon Monoxide, NSRDS–NBS5, U.S. Government Printing Office (Washington, 1966).
47) Locht, R. and Momigny, J., Internat. J. Mass Spectrom. Ion Phys. **7** (1971) 121.
48) Moddeman, W. E., Carlson, T. A., Krause, M. O., Pullen, B. P., Bull, W. E. and Schweitzer, G. K., J. chem. Phys. **55** (1971) 2317.
49) Dorman, F. H. and Morrison, J. D., J. chem. Phys. **35** (1961) 575.
50) Hurley, A. C., J. chem. Phys. **54** (1971) 3656.
51) Newton, A. S. and Sciamanna, A. F., J. chem. Phys. **53** (1970) 132.
52) Advances in Atomic and Molecular Physics, Vol. 2, Acad. Press (New York, London, 1966) p. 177.
53) Schram, B. L., Thesis, University of Amsterdam (1966) p. 83.

IONIZATION OF N_2 AND CO BY 10 keV ELECTRONS
AS A FUNCTION OF THE ENERGY LOSS
II. INNER-SHELL ELECTRONS

M. J. VAN DER WIEL and TH. M. EL-SHERBINI

FOM-Instituut voor Atoom- en Molecuulfysica, Amsterdam, Nederland

Synopsis

Oscillator-strength spectra are reported for the formation of N_2^+, $N^+ + N_2^{++}$ and N^{++}, and CO^+, CO^{++}, C^+, O^+ and C^{++} following N_K excitation in N_2 and C_K excitation in CO. For promotion of a K electron to the first bound molecular-level broad absorption bands are observed both in N_2 and CO, which we ascribe to vibrational excitation. From a comparison with photoabsorption data we infer that the major fraction of K-ionization events leads to dissociation with excess kinetic energy of the fragments. No hydrogen-like jump is recorded at the K edges in N and C. We discuss results obtained in Auger-electron and photoelectron spectroscopy, which are relevant for the present work.

1. *Introduction.* In recent years a considerable amount of new information on excitation of inner-shell electrons in molecules has been gained through the use of X-ray photoelectron [1, 2]) and Auger-electron spectroscopy [1, 3–6]). Such studies have led to a rather detailed knowledge of level energies of intermediate hole states and final (mostly doubly ionized) states, as well as of the associated Auger-decay probabilities. Moreover, excitations of inner-shell electrons to discrete or continuous molecular levels can be distinguished from each other by proper choice of the projectile, *i.e.* photons or electrons [4]). It is evident that in some cases additional information on these processes is provided by a measurement of the photoabsorption [7]) or photoionization spectrum. However, experiments of this type are rather scarce owing to the lack of suitable photon sources.

The experiment described in this paper produces results similar to those of the photoionization type. From the small-angle, inelastic scattering of 10 keV electrons in N_2 and CO, observed in coincidence with the ions, we derive oscillator strengths for ionization to each of the final m/e values. The purpose of the present work is threefold: firstly, to attempt, in continuation of our earlier work on this problem [8, 9]), to clarify certain inconsistencies in previous studies of the discrete inner-shell excitation of N_2 and CO; secondly, to measure, or actually set a lower limit to, the fraction of initial energy

absorption leading to dissociative ionization; thridly, to determine the contribution of electron shake-off to the decay processes. The experimental arrangement and procedure have been discussed in the preceding paper[10] (referred to as I in the following), and earlier papers[11, 12] in such detail that only results will be given.

2. *Results and discussion.* 2.1. General. Oscillator-strength spectra were recorded for the formation of N_2^+, $N^+ + N_2^{++}$ and N^{++} *via* a K-shell process in N_2 (fig. 1); and for CO^+, CO^{++}, C^+, O^+ and C^{++} *via* a carbon K-shell process in CO (fig. 2). The energy resolution was 0.5 eV fwhm for all spectra except those of N^{++} and C^{++}, which were taken with 2 eV resolution. In CO we only investigated the ionization following C_K processes. Excitation of the O_K shell at 542 eV, though it can be observed in the energy-loss spectrum[8]), does not produce reasonable coincidence spectra, since at such high energy losses the incomplete suppression of all other inelastically scattered electrons gives rise to a strong background on the electron detector and therefore raises the number of accidental coincidences.

In each of the spectra of figs. 1 and 2 some discrete structure is present below the K edges. We shall divide the discussion into two parts, one concerning the discrete K-electron excitation and one concerning the part of the spectrum above the K edge. A potential-energy diagram of N_2 and CO is shown in paper I, fig. 9.
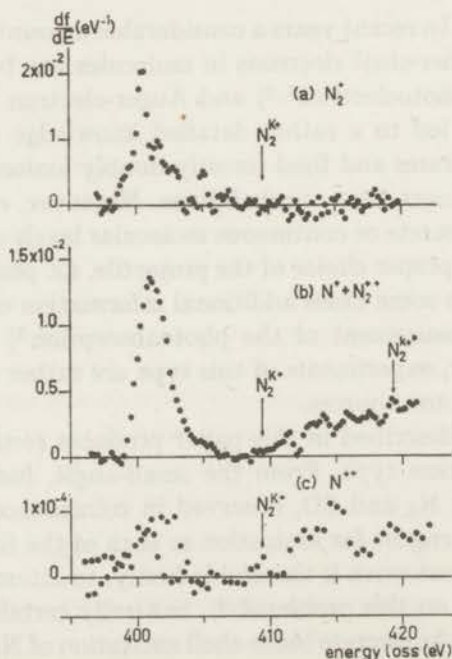

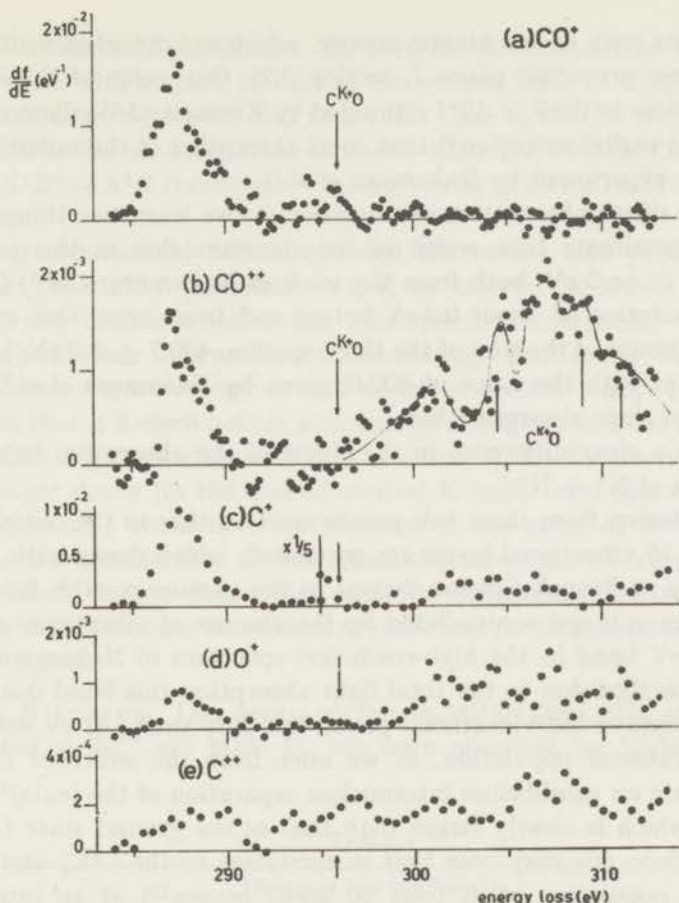Fig. 1. K-shell oscillator-strength spectra of N_2.

Fig. 2. Carbon K-shell oscillator-strength spectra of CO. In the C⁺ spectrum (c) above 295 eV the scale has been enlarged by a factor of 5.

2.2. Discrete K excitation. In this section we confine ourselves to the discussion of the clear, broad peak in the spectra at around 400 eV in N_2 and at 287 eV in CO. In some of the spectra there is an indication of more structure between this peak and the K edge. However, the scatter in the data points does not permit any more detailed conclusions to be drawn. The initial process involved in the large absorption at the peak in the N_2 spectra (fig. 1) has been assigned by Nakamura et al.[7]) to be an excitation of a K electron to the first unoccupied molecular level:

$$(\sigma_u 1s)^2 \dots (\Pi_g 2p)^0, \, X^1\Sigma_g^+ \, (\sigma_u 1s)^1 \dots (\Pi_g 2p)^1, \, {}^1\Pi_u. \quad (1)$$

The total oscillator strength associated with this transition, the sum of the peak areas in fig. 1, is equal to 8×10^{-2}, or 4×10^{-2} per K electron. The value we quote represents a lower limit, as some of the decay may lead to

N^+ fragments with excess kinetic energy, which are detected with reduced efficiency (see preceding paper I, section 2.2). Our value of the oscillator strength is close to the 7×10^{-2} estimated by Krause and Wuilleumier[6]) and confirms the earlier suspicion[8]) that total absorption of the radiation takes place in the experiment by Nakamura et al.[7]).

From the direct observation of transition (1) we learn two things:

a) The approximate base width of the structure due to this excitation appears to be 3 eV, both from the work of Nakamura et al.[7]) (allowing for a resolution of about 0.3 eV fwhm) and from ours. Our energy at the maximum of the sum of the three spectra, 400.7 ± 0.2 eV, is in good agreement with the value of 400.8, given by Nakamura et al.[7]) for the middle of their absorption band.

b) There is a clear difference in the shape of the absorption band of N_2^+ and that of $N^+ + N_2^{++}$.

The conclusion from these two points must be that in the initial process some 10 to 15 vibrational levels are populated, which decay with different distributions of Franck–Condon factors to the various possible final states. This conclusion is not contradicted by the absence of vibrational structure in the 400 eV band in the high-resolution spectrum of Nakamura et al.[7]), since we saw that due to the total light absorption this band does not represent a series of full vibrational peaks, but only their $\frac{1}{2}$–1 eV wide bases. A rich vibrational population, as we infer from the width of the peak, would require an equilibrium internuclear separation of the $(\sigma_u 1s)^1 (\Pi_g 2p)^1$, $^1\Pi_u$ state which is clearly larger than that of the ground state (1.098 Å). For comparison one may note that in excitation to the $C^2\Sigma_u^+$ state a wide vibrational population of at least 10 levels occurs[13]) at an internuclear separation of 1.262 Å. Such a change in this separation shows that the electron removed from the K shell clearly affects the bonding, when promoted to the $\Pi_g 2p$ orbital. This is opposed to the case of a K electron being ionized, for which it has been demonstrated[3]) that almost no effect on the bonding occurs.

For the corresponding excitation in CO, the transition

$$(1s)_C^2 \dots (2\Pi)^0, X^1\Sigma^+ \rightarrow (1s)_C^1 \dots (2\Pi)^1, {}^1\Pi \qquad (2)$$
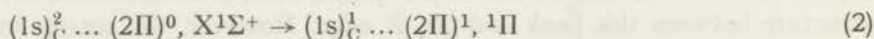
no photoabsorption data exist. However, the present results show that the situation is quite similar to that of N_2. Again we observe in each of the spectra of fig. 2 an absorption band with a base width of about 3 eV, the maximum of the sum of the spectra lying at an energy of (287.3 ± 0.2) eV. The oscillator strength for the discrete C_K excitation, i.e. the sum of the 287 eV peak areas in fig. 2, amounts to 7×10^{-2}, which value we present as a lower limit owing to the possible contribution of energetic fragments. Similarly as in N_2, the width of the absorption band, together with the difference in shape between the CO^{++} and the other spectra, is indicative of

a broad vibrational population. An increase in internuclear separation of the $^1\Pi$-state with respect to that of the ground state of roughly the same magnitude as in N_2, would lead to a value close to that of the $A^2\Pi$ state of CO^+. This seems an acceptable estimate, since the Franck–Condon factors for the $X^1\Sigma^+ \rightarrow A^2\Pi$ transitions[14] also give rise to a wide band of vibrational excitation.

Having summarized and interpreted the earlier and present evidence concerning the initial promotion of a K electron to the lowest bound level, we shall now discuss whether this information is compatible with what is known about these intermediate states through their decay, as observed in Auger-electron spectroscopy as well as in the present study. In general we can state that a K-shell hole in a carbon or nitrogen atom has a probability of less than 1% for decay *via* X-ray emission[15]. By far the most probable is the Auger decay (in the case of neutral K hole states also referred to as auto-ionization), which involves lifetimes of the order of 10^{-14}s. As such lifetimes are considerably shorter than characteristic vibrational times, it follows firstly that no dissociation occurs in the intermediate hole states and secondly that the Auger transitions are confined to the ground-state Franck–Condon region.

2.2.1. Nitrogen. The decay of the $(\sigma_u 1s)^1 (\Pi_g 2p)^1$, $^1\Pi_u$ state (further designated as N_2^{K*} see table I), has been observed by Stalherm *et al.*[3],

TABLE I

Decay of the N_2^{K*} state					
Initial hole state	Decay		Final state	Auger-electron energy	Ion, observed in this work
	Auger transition	Additional-transition			
		—	$X^2\Sigma_g^+$	broad band around 384 eV	
			$A^2\Pi_u$	peak at 383.8 eV	N_2^+
			$B^2\Sigma_u^+$	broad band around 381 eV	
N_2^{K*}: configuration $(\sigma_u 1s)^1 \ldots (\Pi_g 2p)^1$, $^1\Pi_u$	$(\Pi_g 2p)$ el. participates	shake-off	mostly stable N_2^{2+}	351–358 eV	N_2^{2+}
	$(\Pi_g 2p)$ el. remains spectator	—	$C^2\Sigma_u^+$ ($v' \geq 3$ or 4)	373–379 eV	N^+ (little N_2^+)
		shake-off	N_2^{2+} (mostly dissociative); N^{++}		N^+ (with high kinetic energy); N^{++}

Siegbahn *et al.*[1]) and by Carlson *et al.*[4]) in the Auger-electron spectrum in the energy range of 368 to 385 eV, *i.e.* $[E(N_2^{K*})-I.P.(N_2^+)]$. The two most prominent peaks in this range, at 383.8 and 384.7 eV, were ascribed to auto-ionizing transitions (in which the $\Pi_g 2p$ electron participates) to the $A^2\Pi_u$, $v' = 0$ (or 1) and $X^2\Sigma_g^+$, $v' = 0$ states, respectively. However, it is difficult to envisage a potential-energy curve for the N_2^{K*} state, which, although populated over at least 10 vibrational levels, would give rise to transitions to almost exclusively only one vibrational level of two so different N_2^+ states (see *e.g.* the Franck-Condon factors for transitions from the ground state to these two states[13])). In any case the base width of the Auger peak at 384.7 eV is such that it might represent a progression of transitions to the $X^2\Sigma_g^+$ state. Further, the whole range of ejected-electron energies between 368 and 380 eV was shown by Carlson *et al.*[4]) and Moddeman *et al.*[5]) to contain contributions from not further specified higher N_2^+ states. Referring to the proposed internuclear separation of the N_2^{K*} state, *i.e.*, near that of the $C^2\Sigma_u^+$ state, we can understand that decay to the $B^2\Sigma_u^+$ state does not produce a sharp structure; instead, a 3 eV wide population of the N_2^{K*} level should be expected to give rise to a smooth enhancement of the spectrum around 381 eV. Similarly, the broad band of N_2^{K*} vibrational levels could give transitions to almost all vibrational levels of the $C^2\Sigma_u^+$ state. Such transitions would be observed in the Auger spectrum at energies roughly between 373 and 379 eV; *i.e.* the lowest and highest possible energy difference between the N_2^{K*}- and the $C^2\Sigma_u^+$ state. This conclusion is in excellent agreement with observations in the N_2-Auger spectrum (*e.g.* peak 2 of ref. 1). Further evidence that a large fraction of the N_2^{K*} states auto-ionizes to the $C^2\Sigma_u^+$ state is present in our spectra of fig. 1. As discussed in the preceding paper (I), for the higher ($v' \geq 3$ or 4) vibrational levels of the $C^2\Sigma_u^+$ state predissociation occurs. It is evident that these levels will be populated preferentially from high vibrational levels of the N_2^{K*} state. This is then the reason for the difference in shape of the two 400 eV peaks of figs. 1a and 1b. The N^+ band, which apparently for the major part arises from $C^2\Sigma_u^+$ predissociation, has a steeper rise while also its maximum is shifted to higher energy (401.0 eV) with respect to that of the N_2^+ band (400.5 eV).

We must consider which other processes may contribute to the peak of fig. 1b. Mainly this will be decay to stable N_2^{2+} states, *i.e.* Auger decay followed by electron shake-off in which the initially excited electron is ejected (see table I). Such transitions should produce Auger electrons at continuous energies of $(400.7 - \text{I.P. } N_2^{2+}) \text{ eV} = 385.4 \text{ eV}$ and lower. In this energy range some structure exists, which has been ascribed[5]) to simultaneous K- and valency-shell ionization. It is, however, fairly probable that some of the intensity in this range is due to N_2^{2+} formation in view of the amount of CO^{++} formed by the corresponding K excitation in CO (see next section).

As for the N^{++} spectrum (fig. 1c), the statistics is only just sufficient to enable us to conclude that some decay of the N_2^{K*} state yields this final state.

2.2.2. Carbon monoxide. Auger spectra of C_K excitation in CO have been reported by Siegbahn *et al.*[1]) and by Moddeman *et al.*[5]). The vibrational structure in the spectrum of ref. 1 has led to the conclusion that the $C^{K*}O$ state has an internuclear separation close to that of the $B^2\Sigma^+$ state. Apparently only $v' = 0$ of the $C^{K*}O$ state is excited, although Moddeman *et al.*[5]) remark on the possibility of a small population of the $v' = 1$ level. We cannot offer an explanation for the evident conflict between the conclusions from the Auger data and from the width and shape of our absorption peaks (fig. 2).

In the spectrum of CO^{++} (fig. 2b) the peak at 287 eV gives evidence for electron shake-off accompanying the Auger decay. Auger electrons associated with transitions to CO^{++} states [16]) are expected to form a continuum at energies of $(287 - I.P. CO^{++})$ eV $= 245.5$ eV and below. In this energy range some unidentified peaks or onsets of continua are present in the C_K-Auger spectrum [5]), the energies of the structures B-7 and B-10 of ref. 5 being in good agreement with the values expected for decay to the $X^3\Pi$, respectively $A^3\Pi$ state of CO^{++} [16]). In fig. 2b we observe that the onset of the 287 eV absorption band is clearly steeper and also shifted to higher energy than that of the other spectra. In terms of our interpretation of the width of the 287 eV peaks this indicates that only the higher vibrational levels of the $C^{K*}O$ state decay to stable CO^{++} states, or alternatively that the lower vibrational levels are depopulated preferentially by transitions to CO^+ or dissociative states $(C^+, O^+$ and C^{++}, figs. 2c–2e). From the height of the CO^{++} peak relative to that of CO^+, which is of a reasonable order of magnitude [12]) for electron shake-off ($\approx 10\%$), we do not expect that dissociation of CO^{++} into C^+ and O^+ gives a large contribution to the C^+ and O^+ peaks. The fact that the C^+ peak is much higher than that of O^+ could be explained by realizing that after C_K excitation those electrons are mostly involved in the decay, whose orbitals are centered on the atom with the initial K vacancy. The same argument holds for C^{++}. We observe a peak for this fragment, whereas no contribution of O^{++} could be detected.

2.3. K ionization. At energy transfers above the K edge (at 409.5 eV for N_2 and at 295.9 eV for carbon in CO[1])) the most probable decay process is the ordinary Auger transition leading to a doubly charged molecule or two charged fragments. In accord with this, figs. 1 and 2 show the absence of a K continuum in the spectra of the singly charged ions and its presence in all other spectra.

2.3.1. Nitrogen. The most remarkable point of the K continuum of fig. 1b (N^+, N_2^{++}) is the absence of a sharp jump at the K edge followed by

a steady decrease. Such a behaviour might be expected assuming a hydrogenic character of the tightly bound K electrons. However, the calculation of Dalgarno and Parkinson[17]) also does not present a sharp K edge. It is hard to decide on this point in the photoabsorption spectrum of Nakamura *et al.*[7]): firstly, the continuum absorption is already quite close to total absorption and secondly, it is not known whether the quantum yield of the spectrograph is constant over the wavelength range. As for the structures we observe closely above threshold, these could possibly be another occurrence of the phenomenon we observed earlier in Ar. L-shell ionization in Ar at low excess energy above the L edge appeared to result in rapidly varying ratios of "branching" over the various decay channels. The jump at 419 eV can be identified with the onset of simultaneous excitation in inner and valency shell (N_2^{K+*}), according to the energy determination of satellite K-photoelectron lines by Moddeman[2]).

The height of the $N^+ + N_2^{++}$ continuum, which represents the whole K continuum since the contribution of N^{++} is very small, amounts to about 3×10^{-3} eV^{-1}. From a compilation of photoabsorption data by Henke and Elgin[18]) it is known that the increase in oscillator strength across the K edge should be 6.3×10^{-3} eV^{-1} per N atom, or 1.26×10^{-2} eV^{-1} per N_2 molecule. The fact that our value is lower indicates that apparently some K ionization leads to transitions to dissociative N_2^{++} states with a considerable amount of excess energy. The same conclusion was reached by Powell *et al.*[19]) from measurements of the distribution of charged products due to irradiation of N_2 with 1.5 keV X rays. They quote a production of 71% ions with kinetic energy against 29% thermal-energy ions (the latter fraction being subdivided into 35% N_2^+ and 62% N^+, N_2^{++}). However, it seems that their fraction of dissociative ions should be still higher, since with the ratios mentioned the amount of N_2^+ (10% of the total number of ions) formed by 1.5 keV X rays is much higher than what can be derived from other sources. For instance, in the X-ray photoelectron spectrum of Siegbahn *et al.*[1]) the valency-shell lines only have 5% of the intensity of the K-shell line. Moreover, an extrapolation of the nitrogen L-absorption data[18]) to 1.5 keV also yields an oscillator strength of roughly 5% of that of the K shell. The deviation in the results of Powell *et al.*[19]) is possibly due to contamination of the incident radiation with low-energy photons which only produce N_2^+.

2.3.2. Carbon monoxide. Carbon K ionization in CO leads to the production of the ions CO^{++}, C^+, O^+ and C^{++} (see fig. 2). Similarly as in the case of N_2 we do not observe a hydrogen-like absorption maximum at the K edge in the CO^{++}, C^+ and O^+ spectra. A number of the structures in the CO^{++} spectrum appear to occur at energies (see lines in fig. 2b) in accordance with those for simultaneous processes in valency and K shell ($C^{K+*}O$), as measured by Moddeman[2]). These structures seem to be superimposed on

the normal K continuum which has a height of the order of 1×10^{-3} eV^{-1}. Comparing this with earlier values of the C_K absorption jump[18, 20] of about 1×10^{-2} eV^{-1}, we must conclude that the major fraction of C_K ionizing events leads to dissociation. Such a dissociation of CO^{++} states into $(C^+ + O^+)$ with a half-life of less than 10^{-8}s was already observed in the preceding paper (I) after excitation from the ground state. The same holds for transitions from the intermediate C^{K+O} level: Above the K-edge the spectra of C$^+$ and O$^+$ show continua of roughly similar shape and intensity, the C$^+$ continuum being slightly lower owing to the higher velocity and consequently lower collection efficiency of this fragment. Since in most of the known possibilities[16] for dissociation of CO^{++} at least 5 eV kinetic energy is available for the two fragments, the true K-continuum oscillator strength will indeed be considerably larger than that given by the summation over the continua of fig. 2.

As regards the experiment of Powell et al.[19] with 1.5 keV X rays incident on CO, a direct comparison cannot be made since in their case both the C_K and O_K shells can be ionized. However, they mention a fraction of less than 40% of thermal ions, of which 55%, i.e. 22% of the total, are CO$^+$ ions. As in the case of N$_2$, this fraction is anomalously high, when considering the extrapolated valency-shell absorption[18] at 1.5 keV, which amounts to only 5% of that of the two K shells. The same fraction, about 5%, can be derived from the photoelectron spectrum of Siegbahn et al.[1] by taking the intensity ratio of outer-shell lines to that of the K-shell lines. The conclusion of Powell et al.[19] that the group of thermal-energy ions mainly consists of CO^{++} is in agreement with the present data.

The spectrum of fig. 2e is just sufficiently detailed to show that some C^{++} formation takes place above the K edge, whereas no significant O^{++} contribution could be measured. This fact confirms the earlier mentioned atomic picture of the molecule, in which the orbitals centered on the atom with the initial vacancy undergo most of the additional electron shake-off.

3. *Conclusion.* The study of ion formation in N$_2$ and CO as a function of the energy transfer in the K-shell range provides information which is complementary to that from Auger-electron and photoelectron spectrometry. The major conclusion from the present work is that promotion of a K electron to a bound molecular level gives rise to a wide band of vibrational excitation. While in the case of N$_2$ this may be reconciled with the findings in Auger spectrometry, there is an evident discrepancy in the case of CO. Further, we observed that no sharp K jump occurs at the edges in nitrogen and carbon.

Finally, most of the discussion in this paper had to be of a qualitative nature, owing to the unknown kinetic energies of the fragment ions. Further effort in this field should be directed towards determination of these frag-

ment energies, with retention of the potentialities of the electron–ion coincidence technique.

REFERENCES

1) Siegbahn, K., Nordling, C., Johannson, G., Hedman, J., Hedén, P. F., Hamrin, K., Gelius, U., Bergmark, T., Werme, L. O., Manne, R. and Bear, Y., ESCA Applied to Free Molecules, North-Holland Publ. Comp. (Amsterdam, 1969).
2) Moddeman, W. E., Thesis, University of Tennessee, 1970, unpublished.
3) Stalherm, D., Cleff, B., Hillig, H. and Mehlhorn, W., Z. Naturforsch. **24a** (1969) 1728.
4) Carlson, T. A., Moddeman, W. E., Pullen, B. P. and Krause, M. O., Chem. Phys. Letters **5** (1970) 390.
5) Moddeman, W. E., Carlson, T. A., Krause, M. O., Pullen, B. P., Bull, W. E. and Schweitzer, G. K., J. chem. Phys. **55** (1971) 2317.
6) Krause, M. O. and Wuilleumier, F., Oak Ridge National Lab., Chemistry Division Annual Report, May (1971).
7) Nakamura, M., Sasanuma, M., Sato, S., Watanabe, M., Yamashita, H., Iguchi, Y., Ejiri, A., Nakai, S., Yamaguchi, S., Sagawa, T., Nakai, Y. and Oshio, T., Phys. Rev. **178** (1969) 80.
8) Van der Wiel, M. J., El-Sherbini, Th. M. and Brion, C. E., Chem. Phys. Letters **7** (1970) 161.
9) El-Sherbini, Th. M. and Van der Wiel, M. J., Book of Abstracts of VIIth ICPEAC, North-Holland Publ. Comp. (Amsterdam, 1971), p. 1050.
10) El-Sherbini, Th. M. and Van der Wiel, M. J., Physica *xx* (1972) *xxx*.
11) Van der Wiel, M. J., Physica **49** (1970) 411.
12) Van der Wiel, M. J. and Wiebes, G., Physica **53** (1971) 225.
13) Nicholls, R. W., J. quant. Spectrosc. radiat. Transfer **2** (1962) 433.
14) Krupenie, P. H., The Band Spectrum of Carbon Monoxide, U.S. Government Printing Office, Wash. DC (1966).
15) Fink, R. W., Jopson, R. C., Mark, H. and Swift, C. D., Rev. mod. Phys. **38** (1966) 513.
16) Hurley, A. C., J. chem. Phys. **54** (1971) 3656.
17) Dalgarno, A. and Parkinson, D., J. Atmospheric Terrest. Phys. **18** (1960) 335.
18) Henke, B. L. and Elgin, R. L., Advances in X-Ray Analysis, Vol. 13, Plenum Press (New York, 1969).
19) Powell, F. W., Van Brunt, R. J. and Whitehead, W. D., Book of Abstracts of VIIth ICPEAC North-Holland Publ. Comp. (Amsterdam, 1971), p. 152; and private communication.
20) Lukirskii, A. P., Brytov, I. A. and Zimkina, T. M., Optika i. Spectrosk., English Transl. **17** (1964) 234.

94

The work described in this thesis is dealing with the study of inelastic scattering of fast electrons by Kr, Xe, N_2 and CO and the corresponding ionization and fragmentation. The method we used for this study is measuring the energy loss of 10 keV electrons scattered at small angles by the target gas in coincidence with the ion products in the mass spectrometer. Then the measured cross sections for inelastic electron scattering are converted into optical oscillator strengths. Thus in this experiment a source of 0-500 eV photons is simulated by small angle inelastic scattering of 10 keV electrons.

In Chapter I, a general introduction and description of the apparatus are given together with a discussion of some experimental procedures.

In Chapter II, a study of the two noble gases Kr and Xe is made. In Part (A), total electron impact cross sections are determined for the formation of singly and multiply charged ions in the energy range between 2 and 14 keV. The ion selection is performed in a charge analyzer of 100% transmission. In Part (B), oscillator strength spectra are obtained for the formation of $Kr^{1+ - 4+}$ following ionization in the N- and M shells of Kr, and of $Xe^{1+ - 4+}$ following ionization in the O- and N shells of Xe. The spectra of Kr^{1+} and Xe^{1+} show the presence of a minimum followed by a maximum in the contribution of 4p-εd and 5p-εd transitions in Kr and Xe respectively. The nd-εf transitions in Kr and Xe are observed as delayed maxima in the decay to 2+ and 3+ ions. These delayed maxima are due to the presence of a centrifugal potential barrier for the ejection of a 3d electron in Kr and a 4d electron in Xe. Besides interaction between electrons of the outer shell, the results also show the existance of strong direct interaction between electrons of the outer- and first inner shells of Kr and Xe. This electron correlation which is not considered in the calculations is responsible for the discrepancy between experimental results of the oscillator strengths and those predicted by theory.

In Chapter III, a study of the two isoelectronic diatomic molecules N_2

and CO is made. Oscillator-strength spectra for the production of N_2^+, $N^+(N_2^{++})$, CO^+, C^+, O^+ and CO^{++} via ionization in the outer shells of the two molecules are presented in Part (A) of this chapter. The results show that:

a) double electron transitions contribute with a considerable fraction to the N_2^+ oscillator-strength spectrum;

b) N_2^{++} contribution to the m/e = 14 spectrum of N_2 is observed above 42 eV;

c) most of the doubly charged ions (CO^{++}) dissociate to C^+ and O^+ with lifetimes shorter than about 10^{-8} sec.

In Part (B), oscillator-strength spectra for the formation of N_2^+, $N^+ + N_2^{++}$ and N^{++}, and CO^+, CO^{++}, C^+, O^+ and C^{++} following N_K excitation in N_2 and C_K excitation in CO are presented. The results show that the promotion of a K electron to a bound molecular level gives rise to a wide band of vibrational excitation. Concerning ionization, no hydrogen-like shape for the K edges of nitrogen and carbon is observed.

ACKNOWLEDGEMENTS

CURRICULUM VITAE

I was born in Cairo (Egypt) on December 18, 1942. After finishing
the secondary school in 1959, I attended the Faculty of Engineering at
Alexandria University, and received the Bachelors degree in 1964.

Since 1964, I was working at the National Research Centre of Cairo as
a research assistant in the X-ray crystallographic division, under the
guidance of Prof. Dr. M.S. Farag. I was primarily engaged in an X-ray
crystallographic study of some Egyptian minerals in relation to their
use as ceramic resistors and capacitors, which resulted in obtaining
the Masters degree in 1967 from the University of Alexandria.

In March 1968 I obtained a scholarship from the Dutch Ministry of
Foreign Affairs to continue my study for the Doctors degree at the
FOM-Institute for Atomic and Molecular Physics in Amsterdam, under the
supervision of Prof. Dr. J. Kistemaker. At this Institute I started to
do experimental research work on multiple ionization of noble gases by
fast electrons.

In March 1969 I got the degree of "Doctorandus in de Wiskunde en
Natuurkunde" at Leyden University.